The evolution of Hooke's law due to texture development in FCC polycrystals

T. Böhlke, A. Bertram [*]

Institute of Mechanics, Otto-von-Guericke-University of Magdeburg, Postfach 4120, 39016 Magdeburg, Germany

In memory of E.T. Onat

Abstract

Initially isotropic aggregates of crystalline grains show a texture-induced anisotropy of both their inelastic and elastic behavior when submitted to large inelastic deformations. The latter, however, is normally neglected, although experiments as well as numerical simulations clearly show a strong alteration of the elastic properties for certain materials. The main purpose of the work is to formulate a phenomenological model for the evolution of the elastic properties of cubic crystal aggregates. The effective elastic properties are determined by orientation averages of the local elasticity tensors. Arithmetic, geometric, and harmonic averages are compared. It can be shown that for cubic crystal aggregates all of these averages depend on the same irreducible fourth-order tensor, which represents the purely anisotropic portion of the effective elasticity tensor. Coupled equations for the flow rule and the evolution of the anisotropic part of the elasticity tensor are formulated. The flow rule is based on an anisotropic norm of the stress deviator defined by means of the elastic anisotropy. In the evolution equation for the anisotropic part of the elasticity tensor the direction of the rate of change depends only on the inelastic rate of deformation. The evolution equation is derived according to the theory of isotropic tensor functions. The transition from an elastically isotropic initial state to a (path-dependent) final anisotropic state is discussed for polycrystalline copper. The predictions of the model are compared with micro–macro simulations based on the Taylor–Lin model and experimental data. © 2001 Elsevier Science Ltd. All rights reserved.

1. Introduction

The main purpose of the work is to formulate a phenomenological model for the evolution of the elastic properties of polycrystals due to crystallographic texture development. Many materials are aggregates of crystals and exhibit a non-uniform distribution of crystal orientations. Furthermore, technological or natural processes may change the orientation distribution if the deformations are sufficiently large. Deviations

---

[*] Corresponding author. Tel.: +49-391-67-18062; fax: +49-391-67-12863.

E-mail address: bertram@mb.uni-magdeburg.de (A. Bertram).

Nomenclature

f	crystallite orientation distribution function
g	element of Orth
G_α	material function
I_p	determinant of $\widetilde{\mathbf{N}}'_\mathrm{p}$
ζ	parameter in the effective stiffness tensor
η	parameter in the macroscopic flow rule
λ	eigenvalue of the stiffness tensor
ξ	scalar for the parameterization of the stretching tensor
$\{\mathbf{e}_i\}$	orthonormal basis
$\{\mathbf{g}_i\}$	lattice vectors
$\mathbf{B}_\alpha$	orthonormal basis of symmetric second-order tensors
$\mathbf{B}$	left Cauchy–Green tensor
$\mathbf{C}$	right Cauchy–Green tensor
$\mathbf{D}$	stretching tensor
$\widetilde{\mathbf{D}}'_\mathrm{p}$	inelastic rate of deformation
$\mathbf{E}$	infinitesimal strain tensor
$\mathbf{E}^\mathrm{A}$	Almansi strain tensor
$\mathbf{E}^\mathrm{G}$	Green strain tensor
$\mathbf{F}$	deformation gradient
$\widetilde{\mathbf{F}}$	elastic portion of the deformation gradient
$\mathbf{I}$	second-order identity tensor
$\mathbf{K}$	flow rule
$\widetilde{\mathbf{N}}'_\mathrm{p}$	direction of the inelastic rate of deformation
$\mathbf{P}$	inelastic transformation
$\mathbf{R}$	proper orthogonal part of the deformation gradient
$\mathbf{S}$	2. Piola–Kirchhoff stress tensor
$\mathbf{T}$	Cauchy stress tensor
$\mathbb{A}'$	anisotropic part of the effective stiffness tensor
$\mathbb{C}$	stiffness tensor
$\mathbb{D}$	anisotropic part of a stiffness tensor with a cubic symmetry
$\mathbb{G}_\alpha$	fourth-order tensor generator
$\mathbb{K}$	evolution equation for the elasticity tensor
$\mathbb{N}$	tensor defining an anisotropic norm
$\mathbb{P}_\alpha$	projector of the elasticity tensor
$\mathbb{P}_1^\mathrm{I}$	isotropic projector (dilatation)
$\mathbb{P}_2^\mathrm{I}$	isotropic projector (distortion)
$\mathbb{S}$	compliance tensor

from a uniform orientation distribution can cause the effective mechanical or physical properties to be anisotropic. Examples are the elastic, thermal, plastic, electric, or magnetic properties of deformed materials (Bunge, 1993; Krempl, 1994; Kocks et al., 1998). A source for such phenomena is a significant anisotropy of the corresponding physical property of the single crystals forming the aggregate. Besides a crystallographic texture development there are other micro-mechanical mechanisms, which may change the effective elastic

properties. For example, changes that are caused by micro-cracks, pores, or voids are usually macroscopically described by damage models (see, e.g., Zheng and Collins, 1998). In the present paper we consider the influence of the crystallographic texture. For polycrystalline metals the elastic behavior can be linearized in some elastic range and described by Hooke's law. As a result, a constitutive model for the description of the texture-induced elastic anisotropy is required to determine the elasticity tensor as a functional of the deformation process.

The changes in the elastic anisotropy of textured polycrystalline materials are of interest for rather different applications. Examples are the spring-back analysis for metal forming processes and the investigation of wave propagation phenomena in geological materials. Moreover, experiments indicate that the effective elastic and (visco)plastic properties are correlated for moderately textured polycrystals (e.g., Stickels and Mould, 1970). Therefore, the anisotropy of the (visco)plastic behavior can be analyzed by investigating the elastic anisotropy.

In the present paper the micro–macro transition is based on orientation averages of the local elastic properties, which do not take into account the interaction of the grains and the geometrical characteristics of the microstructure. This approach, although less accurate than more sophisticated averaging schemes such as the self-consistent estimates or finite element calculations, allows the derivation of simple expressions describing the macroscopic anisotropy in terms of the microstructure and gives a first insight into the dominating mechanisms. The considerations are limited to aggregates of cubic crystals. Based on the harmonic decomposition of elasticity tensors (for an overview see Forte and Vianello, 1996) it is shown that for this material class an irreducible fourth-order tensor having nine independent components completely describes the elastic anisotropy. In order to make the model as simple as possible in a first step, coaxial deformation processes are considered that can be described by a symmetric velocity gradient. Examples for such processes are simple tension, plane strain compression, or simple compression.

The outline of the paper is as follows. In Section 2, a brief introduction to the adopted notation is given. In Section 3, the assumption that the elastic properties of single crystals are not affected by inelastic deformations is used to derive the stress–strain relation for single crystals in the elastoplastic case. Moreover, the projector representation of linear anisotropic elastic properties is briefly discussed and specified for the case of cubic crystals. The effective elastic properties of polycrystals are determined by orientation averages of the local elasticity tensors. Arithmetic, geometric, and harmonic averages are compared. It is shown that in the case of cubic constituents the anisotropy of the effective elasticity tensors depends for all of the aforementioned averages on the same a fourth-order tensor. In Section 4, coupled evolution equations for the inelastic transformation and the anisotropic part of the elasticity tensor are formulated. Guided by experimental findings, Man (1995) formulated a quadratic yield function assuming that the elastic and plastic properties are correlated linearly. The authors adopt this approach and formulate a viscoplastic flow rule, which is based on an anisotropic norm of the stress deviator defined by means of the anisotropic part of the elasticity tensor. The growth law for this anisotropic part is derived assuming that the direction of the rate of change only depends on the inelastic rate of deformation. In Section 5, a parameterization of traceless and symmetric second-order tensors is presented that allows for a systematic classification of the deformation modes considered. The transition from an elastically isotropic initial state to a path-dependent final anisotropic state is discussed for polycrystalline copper. The predictions of the model are compared with micro–macro simulations based on the Taylor–Lin model (Taylor, 1938; Lin, 1957) and experiments (Weerts, 1933; Alers and Liu, 1967).

2. Notation

Throughout the text a direct tensor notation is preferred. In order to avoid additional formal definitions, the index notation is applied in some cases using the summation convention. A linear mapping of a

second-order tensor is written as $\mathbf{A} = \mathbb{C}[\mathbf{B}]$. The scalar product, the dyadic product, and the Frobenius norm are denoted by $\mathbf{A} \cdot \mathbf{B}$, $\mathbf{A} \otimes \mathbf{B}$, and $\|\mathbf{A}\| = (\mathbf{A} \cdot \mathbf{A})^{1/2}$, respectively. Sym, Psym, Orth, and Inv represent the sets of symmetric, symmetric and positive-definite, proper orthogonal, and invertible second-order tensors. Irreducible, i.e., completely symmetric and traceless tensors are designated by a prime, e.g., $\mathbf{A}'$ and $\mathbb{C}'$. The symmetric and the skew-symmetric parts of a second-order tensor $\mathbf{A}$ are denoted by $\text{sym}(\mathbf{A})$ and $\text{skw}(\mathbf{A})$, respectively. The Rayleigh product $\mathbf{A} \times \mathbb{C}$ of a fourth-order tensor $\mathbb{C} = C_{ijkl}\mathbf{e}_i \otimes \mathbf{e}_j \otimes \mathbf{e}_k \otimes \mathbf{e}_l$ and a second-order tensor $\mathbf{A}$ is defined by

$$\mathbf{A} \times \mathbb{C} = C_{ijkl}\mathbf{A}\mathbf{e}_i \otimes \mathbf{A}\mathbf{e}_j \otimes \mathbf{A}\mathbf{e}_k \otimes \mathbf{A}\mathbf{e}_l, \tag{1}$$

where $\{\mathbf{e}_i\}$ is an orthonormal basis. If $\mathbb{C}$ exhibits a symmetry in the first or second pair of indices (e.g., $C_{ijkl} = C_{jikl}$) or the major symmetry ($C_{ijkl} = C_{klij}$), $\mathbf{A} \times \mathbb{C}$ shows the same symmetry properties for all $\mathbf{A}$. The associativity $\mathbf{A} \times (\mathbf{B} \times \mathbb{C}) = (\mathbf{A}\mathbf{B}) \times \mathbb{C}$ holds for all second-order tensors $\mathbf{A}$ and $\mathbf{B}$. Denoting the material derivative by a dot, a Lie derivative of the Oldroyd-type (Oldroyd, 1950; Marsden and Hughes, 1983) of an objective tensor fourth-order tensor $\mathbb{C}$ can be expressed as

$$\mathscr{L}(\mathbb{C}, \mathbf{A}) = \mathbf{A} \times (\mathbf{A}^{-1} \times \mathbb{C})^{\bullet}. \tag{2}$$

3. Elastic properties of single crystals and polycrystals

3.1. Single crystals: materials with isomorphic elastic ranges

The reduced form of an elastic law $\mathbf{S} = \mathbf{h}(\mathbf{C})$ is used for the description of the single crystal elastic behavior, with $\mathbf{S} = \mathbf{F}^{-1}J\mathbf{T}\mathbf{F}^{-T}$ the 2.Piola–Kirchhoff stress tensor and $\mathbf{T}$ the Cauchy stress tensor. $\mathbf{F}$ denotes the deformation gradient, J the determinant of $\mathbf{F}$, and $\mathbf{C} = \mathbf{F}^{T}\mathbf{F}$ the right Cauchy–Green tensor, respectively. The function $\mathbf{h}$ is invariant under changes of the observer and depends on the current elastic range. In order to specify this dependence, it is assumed that the elastic behavior of the single crystal on the microscale is not affected by inelastic deformations. This assumption is motivated by the microphysical mechanisms of inelastic and elastic deformations in single crystals at room temperature. The latter are found to be reversible deformations of the lattice, and thus unaffected by the dislocation movement, which contributes to the inelastic deformations.

The assumption of constant elastic properties is equivalent to the following statement. Let $\mathbf{h}$ and $\tilde{\mathbf{h}}$ be two elastic laws of the same material point corresponding to elastic ranges before and after an inelastic deformation, then $\mathbf{h}$ and $\tilde{\mathbf{h}}$ are isomorphic, i.e., there exists a material isomorphism $\mathbf{P} \in \text{Inv}$ such that

$$\mathbf{h}(\mathbf{C}) = \mathbf{P}\tilde{\mathbf{h}}(\mathbf{P}^{T}\mathbf{C}\mathbf{P})\mathbf{P}^{T} \tag{3}$$

holds for all $\mathbf{C} \in \text{Psym}$ (Bertram, 1992, 1999). As a result, the current elastic law can be represented by a (constant) referential elastic law $\tilde{\mathbf{h}}$ and a second-order tensor $\mathbf{P} \in \text{Inv}$, called plastic or inelastic transformation. Without loss of generality, the reference law is formulated with respect to the undistorted state of the solid (Truesdell and Noll, 1965, p. 82). The tilde shall indicate that the function is formulated with respect to the undistorted state, which is characterized by the fact that corresponding symmetry transformations are elements of Orth.

For a given process of the deformation gradient $\mathbf{F}$, the internal variable $\mathbf{P}$ has to be determined by an evolution equation (flow rule) and initial conditions. From Eq. (3) it is clear that the orthogonal part of $\mathbf{P}$ (determined by the polar decomposition) can be dropped if the elastic referential law $\tilde{\mathbf{h}}$ is isotropic. If the function $\tilde{\mathbf{h}}$ is anisotropic, however, a non-symmetric internal variable $\mathbf{P}$ is generally necessary. For the

non-uniqueness of $\mathbf{P}$ due to the symmetry properties of $\tilde{\mathbf{h}}$ (see Bertram, 1999). By identifying the so called plastic deformation gradient $\mathbf{F}_{\mathrm{p}} \equiv \mathbf{P}^{-1}$, one can derive the well-known stress–strain relations based on the multiplicative decomposition of the deformation gradient into an elastic and a plastic part. Therefore, the aforementioned approach supports the formula that is used within this context.

To model the elastic ranges of metals, physically linear laws are sufficient for the description of elasticity. If the linearization is carried out with respect to the undistorted state, then one obtains

$$\mathbf{S} = \mathbf{P}\widetilde{\mathbb{C}}[\tfrac{1}{2}(\mathbf{P}^{\mathrm{T}}\mathbf{C}\mathbf{P} - \mathbf{I})]\mathbf{P}^{\mathrm{T}}. \tag{4}$$

Starting with Eq. (4) and defining $\widetilde{\mathbf{F}} = \mathbf{F}\mathbf{P}$, $\widetilde{J} = \det(\widetilde{\mathbf{F}})$, and $\widetilde{\mathbf{S}} = \widetilde{\mathbf{F}}^{-1}\widetilde{J}\mathbf{T}\widetilde{\mathbf{F}}^{-\mathrm{T}}$, three equivalent formulations of the elastic law can be derived

$$\begin{aligned}
\widetilde{\mathbf{S}} &= \widetilde{\mathbb{C}}[\widetilde{\mathbf{E}}^{\mathrm{G}}], \quad \widetilde{\mathbf{E}}^{\mathrm{G}} = \tfrac{1}{2}(\widetilde{\mathbf{F}}^{\mathrm{T}}\widetilde{\mathbf{F}} - \mathbf{I}), \\
\mathbf{S} &= \mathbb{C}[\mathbf{E}^{\mathrm{G}} - \mathbf{E}_{\mathrm{U}}^{\mathrm{G}}], \quad \mathbf{E}_{\mathrm{U}}^{\mathrm{G}} = \tfrac{1}{2}(\mathbf{P}^{-\mathrm{T}}\mathbf{P}^{-1} - \mathbf{I}), \\
\boldsymbol{\tau} &= \mathbb{C}_{\mathrm{E}}[\mathbf{E}^{\mathrm{A}} - \mathbf{E}_{\mathrm{U}}^{\mathrm{A}}], \quad \mathbf{E}_{\mathrm{U}}^{\mathrm{A}} = \mathbf{F}^{-\mathrm{T}}\mathbf{E}_{\mathrm{U}}^{\mathrm{G}}\mathbf{F}^{-1},
\end{aligned} \tag{5}$$

where $\boldsymbol{\tau} = J\mathbf{T}$ denotes the Kirchhoff stress tensor. The first expression in Eq. (5) represents the elastic law with respect to the undistorted state and gives the simplest formula because of the constant reference stiffness $\widetilde{\mathbb{C}}$. The second expression in Eq. (5) gives the elastic law with respect to an arbitrary but fixed reference placement, that does not necessarily coincide with the initial placement. The third expression in Eq. (5) represents the Eulerian form of the elastic law, which is objective but not invariant under Euclidean transformations. The index 'E' is used to denote Eulerian variables and functions. In contrast to the path-independent stiffness tensor $\widetilde{\mathbb{C}}$, the corresponding quantities with respect to the reference and current placement are generally path-dependent

$$\mathbb{C} = \mathbf{P} \times \widetilde{\mathbb{C}}, \quad \mathbb{C}_{\mathrm{E}} = \widetilde{\mathbf{F}} \times \widetilde{\mathbb{C}} = \mathbf{F} \times \mathbb{C}. \tag{6}$$

The strain measure $\widetilde{\mathbf{E}}^{\mathrm{G}}$ symbolizes the Green strain tensor with regard to the undistorted state. $\mathbf{E}^{\mathrm{G}}$ and $\mathbf{E}^{\mathrm{A}}$ are the Green and Almansi strain tensors.

The fourth-order stiffness tensor $\widetilde{\mathbb{C}}$ and the corresponding compliance tensor $\widetilde{\mathbb{S}}$ are specified by the symmetry group $\widetilde{S}$ of the material with regard to the undistorted state, e.g., in terms of stiffnesses

$$\widetilde{\mathbb{C}} = \widetilde{\mathbf{H}} \times \widetilde{\mathbb{C}}, \quad \forall \widetilde{\mathbf{H}} \in \widetilde{S} \subseteq \mathrm{Orth}. \tag{7}$$

The elements of the symmetry group of the Eulerian representation are determined by the elements of $\widetilde{S}$ through a transformation by $\widetilde{\mathbf{F}}$

$$\mathbb{C}_{\mathrm{E}} = \mathbf{H}_{\mathrm{E}} \times \mathbb{C}_{\mathrm{E}}, \quad \forall \mathbf{H}_{\mathrm{E}} \in \widetilde{\mathbf{F}}\widetilde{S}\widetilde{\mathbf{F}}^{-1}. \tag{8}$$

From Eq. (8) one concludes

$$\mathbf{H}_{\mathrm{E}} = \widetilde{\mathbf{R}}\widetilde{\mathbf{H}}\widetilde{\mathbf{R}}^{-1} + \mathcal{O}(\|\widetilde{\mathbf{E}}^{\mathrm{G}}\|), \tag{9}$$

where $\widetilde{\mathbf{R}}$ is the orthogonal part of $\widetilde{\mathbf{F}}$. As a result, the symmetry groups $\widetilde{S}$ and S_{E} are related by $S_{\mathrm{E}} \approx \widetilde{\mathbf{R}}\widetilde{S}\widetilde{\mathbf{R}}^{-1}$, if the elastic strains are small, i.e. $\|\widetilde{\mathbf{E}}^{\mathrm{G}}\| \ll 1$.

For hyperelastic materials the elasticity tensors possess the major symmetry. The symmetry in the first and last pair of indices is assumed as usual. Because of the major symmetry of the elasticity tensors, the following projector representations exist (Halmos, 1958; Rychlewski and Zhang, 1989; Bertram and Olschewski, 1991; Rychlewski, 1995)

$$\widetilde{\mathbb{C}} = \sum_{\alpha=1}^{\beta} \lambda_{\alpha}\mathbb{P}_{\alpha}, \qquad \widetilde{\mathbb{S}} = \sum_{\alpha=1}^{\beta} \frac{1}{\lambda_{\alpha}}\mathbb{P}_{\alpha}. \tag{10}$$
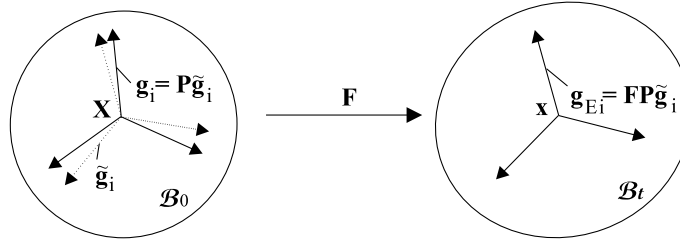
Fig. 1. The deformation gradient $\mathbf{F}$ maps material tangent vectors from the reference placement of the body $\mathcal{B}_0$ to the current placement $\mathcal{B}_t$. The inelastic transformation $\mathbf{P} = \mathbf{g}_i \otimes \widetilde{\mathbf{g}}^i$ maps the Lagrangian reference lattice vectors $\widetilde{\mathbf{g}}_i = \mathbf{g}_i(t = 0)$ onto the current Lagrangian lattice vectors $\mathbf{g}_i(t)$. The Eulerian vectors are obtained by the mapping $\mathbf{g}_{\mathrm{E}i} = \mathbf{F}\mathbf{g}_i$. The transformation of the elasticity tensors follows the same rule (see Eq. (6)).

Here, β $(2 \leqslant \beta \leqslant 6)$ is the number of distinct eigenvalues λ_α of $\widetilde{\mathbb{C}}$. The projectors $\mathbb{P}_\alpha$ are idempotent $\mathbb{P}_\alpha \mathbb{P}_\alpha = \mathbb{P}_\alpha$, biorthogonal $\mathbb{P}_\alpha \mathbb{P}_\beta = \mathbb{O}$ $(\alpha \neq \beta)$, and complete $\sum_{\alpha=1}^{\beta} \mathbb{P}_\alpha = \mathbb{I}$ with $\mathbb{I}$ the identity on symmetric second-order tensors.

In the case of isotropy, there are two distinct eigenvalues $(\beta = 2)$, and the corresponding projectors are given by

$$\mathbb{P}_1^{\mathrm{I}} = \tfrac{1}{3}\mathbf{I} \otimes \mathbf{I}, \qquad \mathbb{P}_2^{\mathrm{I}} = \mathbb{I} - \mathbb{P}_1^{\mathrm{I}}, \tag{11}$$

where $\mathbf{I}$ denotes the second-order identity tensor. In the case of cubic single crystals the elasticity tensors have three distinct eigenvalues $(\beta = 3)$. They are here given by the components of $\widetilde{\mathbb{C}}$ with respect to the orthonormal lattice vectors $\{\widetilde{\mathbf{g}}_i\}$ $(i = 1, 2, 3)$: $\lambda_1 = \widetilde{C}_{1111} + 2\widetilde{C}_{1122}$, $\lambda_2 = \widetilde{C}_{1111} - \widetilde{C}_{1122}$, and $\lambda_3 = 2\widetilde{C}_{1212}$. The cubic projectors are

$$\mathbb{P}_1^{\mathrm{C}} = \mathbb{P}_1^{\mathrm{I}}, \quad \mathbb{P}_2^{\mathrm{C}} = \mathbb{D} - \mathbb{P}_1^{\mathrm{C}}, \quad \mathbb{P}_3^{\mathrm{C}} = \mathbb{I} - \mathbb{P}_2^{\mathrm{C}} - \mathbb{P}_1^{\mathrm{C}}. \tag{12}$$

The anisotropic part $\mathbb{D}$ is given by a dyadic product of lattice vectors

$$\mathbb{D} = \sum_{i=1}^{3} \widetilde{\mathbf{g}}_i \otimes \widetilde{\mathbf{g}}_i \otimes \widetilde{\mathbf{g}}_i \otimes \widetilde{\mathbf{g}}_i. \tag{13}$$

Fig. 1 illustrates how the deformation gradient $\mathbf{F}$ and the inelastic transformation $\mathbf{P}$ act on the lattice vectors of the single crystal.

3.2. Polycrystals: coupling of texture and effective elastic properties

In this section it is assumed that the aggregate is macroscopically and microscopically stress free. By introducing the orientation distribution function f defined on Orth, different orientation averages of elasticity tensors can be introduced. The function f specifies the volume fraction of crystals having an orientation between g and $g + \mathrm{d}g$, i.e. $\mathrm{d}V/V = f(g)\,\mathrm{d}g$. As a result, volume averages can be transformed into averages over Orth and vice versa. The most common mean values are the arithmetic and harmonic mean of the local stiffness tensors, which were first suggested by Voigt and Reuss

$$\widetilde{\mathbb{C}}^{\mathrm{V}} = \int_g f(g)\widetilde{\mathbb{C}}(g)\,\mathrm{d}g, \qquad \widetilde{\mathbb{S}}^{\mathrm{R}} = \int_g f(g)\widetilde{\mathbb{S}}(g)\,\mathrm{d}g \neq \widetilde{\mathbb{C}}^{\mathrm{V}^{-1}}, \tag{14}$$

(Voigt, 1910; Reuss, 1929; Bunge, 1968; Morris, 1969). The arithmetic and harmonic mean correspond to the assumption of homogeneous strain and stress fields, respectively. These approaches give upper and lower bounds for the strain energy density (Hill, 1952; Nemat-Nasser and Hori, 1993). The lower the degree

of the elastic anisotropy on the microscale is, the more accurate they are. Alternative approaches have been developed in order to obtain more precise information from the texture data. Hill (1952) proposed both an arithmetic and a geometric mean of the isotropic bounds by Voigt and Reuss, which give estimates closer to experimental results.

An approach that focuses on a homogenization resulting in unique effective properties, such that the inverse of the mean compliance is equal to the mean stiffness, was given by Aleksandrov and Aisenberg (1966) and further developed by Matthies and Humbert (1995). Here the geometric mean of the local elastic moduli is used

$$\widetilde{\mathbb{C}}^{A} = \exp\left(\int_g f(g)\ln(\widetilde{\mathbb{C}}(g))\,\mathrm{d}g\right), \quad \widetilde{\mathbb{S}}^{A} = \exp\left(\int_g f(g)\ln(\widetilde{\mathbb{S}}(g))\,\mathrm{d}g\right) \equiv \mathbb{C}^{A^{-1}}. \tag{15}$$

Predictions based on this approach are similar to self-consistent estimates and close to experimental data (Matthies and Humbert, 1995).

A uniform distribution of crystal orientations is characterized by the fact that the corresponding distribution function f is constant over its range of definition. This situation is commonly called a grey texture. A uniform distribution of crystal orientations implies only isotropic effective elastic properties if the homogenization is based on the function f alone. Generally, other characteristics of the microstructure may influence the effective properties. Examples are the distributions of grain boundary surfaces, grain edges, or dislocations. It has been shown by Adams et al. (1994) that the grain-boundary structure is the dominant aspect of microstructure affecting bounds of the effective strain energy beyond the distribution of crystal orientations. In the present work we rely on orientation averages. As mentioned before, for a uniform distribution of crystal orientations, $f(g) = 1$ holds for all $g \in$ Orth, and the integrals

$$\widetilde{\mathbb{C}}^{VI} = \int_g \widetilde{\mathbb{C}}(g)\,\mathrm{d}g, \quad \widetilde{\mathbb{C}}^{AI} = \exp\left(\int_g \ln(\widetilde{\mathbb{C}}(g))\,\mathrm{d}g\right), \quad \widetilde{\mathbb{S}}^{RI} = \int_g \widetilde{\mathbb{S}}(g)\,\mathrm{d}g \tag{16}$$

can be expressed solely in terms of the single crystal constants. By introducing the notation

$$\mathbb{C}^{VI} = \lambda_1^{VI}\mathbb{P}_1^{I} + \lambda_2^{VI}\mathbb{P}_2^{I}, \quad \mathbb{C}^{AI} = \lambda_1^{AI}\mathbb{P}_1^{I} + \lambda_2^{AI}\mathbb{P}_2^{I}, \quad \mathbb{C}^{RI} = \lambda_1^{RI}\mathbb{P}_1^{I} + \lambda_2^{RI}\mathbb{P}_2^{I}, \tag{17}$$

and defining the weights $W_{\gamma\alpha}$ by scalar products of the projectors used in Eqs. (10) and (11)

$$W_{\gamma\alpha} = \frac{\mathbb{P}_\gamma^I}{\|\mathbb{P}_\gamma^I\|^2} \cdot \mathbb{P}_\alpha \quad (\gamma = 1, 2; \ \alpha = 1, \ldots, \beta), \tag{18}$$

the eigenvalues of the fourth-order tensors (17) can be written as arithmetic, geometric, and harmonic means of the eigenvalues λ_α with respect to the weights $W_{\gamma\alpha}$

$$\lambda_\gamma^{VI} = \sum_{\alpha=1}^{\beta} W_{\gamma\alpha}\lambda_\alpha, \quad \lambda_\gamma^{AI} = \prod_{\alpha=1}^{\beta} \lambda_\alpha^{W_{\gamma\alpha}}, \quad \frac{1}{\lambda_\gamma^{RI}} = \sum_{\alpha=1}^{\beta} W_{\gamma\alpha}\frac{1}{\lambda_\alpha} \quad (\gamma = 1, 2). \tag{19}$$

The following inequalities are generally valid $\lambda_\gamma^{VI} \geqslant \lambda_\gamma^{AI} \geqslant \lambda_\gamma^{RI}$. The formulation of Eq. (16) in terms of projections onto the space of isotropic linear elastic laws reveals that $\mathbb{C}^{VI}$, $\mathbb{C}^{AI}$, and $\mathbb{S}^{RI}$ solve the minimum problems

$$\begin{aligned}
&\min_{\lambda_1,\lambda_2 \in \mathscr{R}^+} \|\widetilde{\mathbb{C}}^{V} - \lambda_1\mathbb{P}_1^I - \lambda_2\mathbb{P}_2^I\| \iff \lambda_\gamma = \lambda_\gamma^{VI}, \\
&\min_{\lambda_1,\lambda_2 \in \mathscr{R}^+} \|\ln(\widetilde{\mathbb{C}}^{A}) - \ln(\lambda_1)\mathbb{P}_1^I - \ln(\lambda_2)\mathbb{P}_2^I\| \iff \lambda_\gamma = \lambda_\gamma^{AI}, \\
&\min_{\lambda_1,\lambda_2 \in \mathscr{R}^+} \left\|\widetilde{\mathbb{S}}^{R} - \frac{1}{\lambda_1}\mathbb{P}_1^I - \frac{1}{\lambda_2}\mathbb{P}_2^I\right\| \iff \lambda_\gamma = \lambda_\gamma^{RI},
\end{aligned} \tag{20}$$

($\gamma = 1, 2$). Hence, the isotropic estimates by Voigt and Reuss represent the isotropic elastic laws nearest to both the single crystal law (10) and the volume averages (14) (Federov, 1968). Furthermore, one can see that $\ln(\mathbb{C}^{AI})$ minimizes the distance to both $\ln(\mathbb{C})$ and $\int_g \ln(\mathbb{C}(g)) \, dg$ (Böhlke and Bertram, 2000).

Based on the aforementioned formulae it is possible to decompose the (generally anisotropic) averages (14) and (15) into isotropic and anisotropic parts

$$
\begin{aligned}
\widetilde{\mathbb{C}}^{\mathrm{V}} &= \widetilde{\mathbb{C}}^{\mathrm{VI}} + \zeta^{\mathrm{V}} \widetilde{\mathbb{A}}^{\mathrm{V}}, \\
\ln(\widetilde{\mathbb{C}}^{\mathrm{A}}) &= \ln(\widetilde{\mathbb{C}}^{\mathrm{AI}}) + \zeta^{\mathrm{A}} \widetilde{\mathbb{A}}^{\mathrm{A}}, \\
\widetilde{\mathbb{S}}^{\mathrm{R}} &= \widetilde{\mathbb{S}}^{\mathrm{RI}} + \zeta^{\mathrm{R}} \widetilde{\mathbb{A}}^{\mathrm{R}}.
\end{aligned}
\tag{21}
$$

By definition, the norms $\|\widetilde{\mathbb{A}}^{\mathrm{V,A,R}}\|$ are zero for a uniform orientation distribution. The scalars $\zeta^{\mathrm{V,A,R}}$ are defined such that the norms $\|\widetilde{\mathbb{A}}^{\mathrm{V,A,R}}\|$ are equal to one for a single orientation. The orthogonality of the isotropic and anisotropic parts, e.g., $\widetilde{\mathbb{A}}^{\mathrm{V}} \cdot \widetilde{\mathbb{C}}^{\mathrm{VI}} = 0$, causes the following constraints $\widetilde{A}_{iijj}^{\mathrm{V,A,R}} = 0$, $\widetilde{A}_{ijij}^{\mathrm{V,A,R}} = 0$.

Inspection shows that for aggregates of cubic crystals, the scalar factors in Eq. (21) are given by

$$
\zeta^{\mathrm{V}} = \sqrt{\frac{6}{5}}(\lambda_3 - \lambda_2), \quad \zeta^{\mathrm{A}} = \sqrt{\frac{6}{5}}(\ln(\lambda_3) - \ln(\lambda_2)), \quad \zeta^{\mathrm{R}} = \sqrt{\frac{6}{5}}\left(\frac{1}{\lambda_3} - \frac{1}{\lambda_2}\right).
\tag{22}
$$

With Eqs. (11), (12), and (18) one easily determines the weights as

$$
\{W_{1\alpha}\} = \{1, 0, 0\}, \quad \{W_{2\alpha}\} = \left\{0, \frac{2}{5}, \frac{3}{5}\right\}.
\tag{23}
$$

Moreover, from Eqs. (11), (12), (14), and (23) it follows that

$$
\widetilde{\mathbb{A}}^{\mathrm{V}} = \widetilde{\mathbb{A}}^{\mathrm{A}} = \widetilde{\mathbb{A}}^{\mathrm{R}} =: \widetilde{\mathbb{A}}'
\tag{24}
$$

holds and the tensor $\widetilde{\mathbb{A}}'$ can be brought into the form

$$
\widetilde{\mathbb{A}}' = \frac{\sqrt{30}}{30}\left(\mathbf{I} \otimes \mathbf{I} + 2\mathbb{I} - 5\int_g \sum_{k=1}^{3} f(g)\widetilde{\mathbf{g}}_k(g) \otimes \widetilde{\mathbf{g}}_k(g) \otimes \widetilde{\mathbf{g}}_k(g) \otimes \widetilde{\mathbf{g}}_k(g) \, dg\right).
\tag{25}
$$

An equivalent formulation with respect to the arbitrary but fixed orthonormal reference basis $\{\mathbf{e}_i\}$ is obtained by introducing the orthogonal tensor $\mathbf{Q} = \widetilde{\mathbf{g}}_i \otimes \mathbf{e}_i = Q_{ij}\mathbf{e}_i \otimes \mathbf{e}_j$ that maps the basis $\{\mathbf{e}_i\}$ onto the local lattice vectors $\{\widetilde{\mathbf{g}}_i\}$

$$
\widetilde{A}'_{ijmn} = \frac{\sqrt{30}}{30}\left(\delta_{ij}\delta_{mn} + \delta_{im}\delta_{jn} + \delta_{in}\delta_{jm} - 5\int_g \sum_{k=1}^{3} f(g)Q_{ik}(g)Q_{jk}(g)Q_{mk}(g)Q_{nk}(g) \, dg\right).
\tag{26}
$$

The tensor $\widetilde{\mathbb{A}}'$ is irreducible, i.e. completely symmetric and traceless

$$
\widetilde{A}'_{ijkl} = \widetilde{A}'_{jikl} = \widetilde{A}'_{klij} = \widetilde{A}'_{kjil} = \ldots, \qquad \widetilde{A}'_{iikl} = 0.
\tag{27}
$$

Irreducible fourth-order tensors have nine independent components (Boehler et al., 1994). Hence, in the case of aggregates of cubic crystals the effective elastic behavior is completely determined by 11 constants. Two parameters describe the isotropic behavior and the other nine reflect the influence of the crystallographic texture. The reduction of the number of independent elastic constants on the macroscale from 21 (general triclinic) to 11 is thus a direct consequence of the cubic crystal symmetry on the microscale.

Experiments confirm that the tensor $\widetilde{\mathbb{A}}'$ properly represents the elastic anisotropy. Texture data of rolled copper were used to determine the Voigt and Reuss average as well as the Hill approximation of Young's modulus (Alers and Liu, 1966; Kallend and Davies, 1971). The comparison of these predictions with the measured moduli shows that the absolute value of Young's modulus depends strongly on the type of the

average, but the variation of the modulus with respect to the sample geometry is not very sensitive to the special type of the average and corresponds to the observations.

The deviation from the isotropic elastic state can be expressed in terms of stiffnesses and compliances. Starting from Eq. (21) and applying compatible norms for second- and fourth-order tensors, one obtains the following material dependent estimates

$$\frac{\|\widetilde{\mathbb{C}}^{\mathrm{V}} - \widetilde{\mathbb{C}}^{\mathrm{VI}}\|}{\|\widetilde{\mathbb{C}}^{\mathrm{VI}}\|} = f_1 \|\widetilde{\mathbb{A}}'\|, \quad \frac{\|\widetilde{\mathbb{S}}^{\mathrm{R}} - \widetilde{\mathbb{S}}^{\mathrm{RI}}\|}{\|\widetilde{\mathbb{S}}^{\mathrm{RI}}\|} = f_2 \|\widetilde{\mathbb{A}}'\|. \tag{28}$$

As examples for both a weakly and a strongly anisotropic material, the coefficients for aluminum and copper are given: $f_1^{\mathrm{Al}} = 0.043$, $f_2^{\mathrm{Al}} = 0.098$, $f_1^{\mathrm{Cu}} = 0.237$, $f_2^{\mathrm{Cu}} = 0.570$. Therefore, copper exhibits a much more pronounced anisotropy compared to aluminum for identical textures.

The general decomposition (21) and the special properties given by Eqs. (24) and (27) can be interpreted from another point of view. The harmonic decomposition of elasticity tensors into a direct sum of orthogonal subspaces (e.g., Schouten (1924), Cowin (1989), Boehler et al. (1994), for an overview see Forte and Vianello (1996)).

$$\widetilde{\mathbb{C}} = h_1 \mathbb{P}_1^{\mathrm{I}} + h_2 \mathbb{P}_2^{\mathrm{I}} + \widetilde{\mathbf{H}}_1' \otimes \mathbf{I} + \mathbf{I} \otimes \widetilde{\mathbf{H}}_1' + 4\mathbb{J}[\widetilde{\mathbf{H}}_2'] + \widetilde{\mathbb{H}}' \tag{29}$$

holds, where $\widetilde{\mathbf{H}}_1'$, $\widetilde{\mathbf{H}}_2'$, and $\widetilde{\mathbb{H}}'$ are irreducible, i.e., completely symmetric and traceless tensors. For the definition of $\mathbb{J}[\widetilde{\mathbf{H}}_2']$ see Appendix A. h_1 and h_2 are called the first and second isotropic parts; $\widetilde{\mathbf{H}}_1'$ and $\widetilde{\mathbf{H}}_2'$ are the first and second deviatoric parts; $\widetilde{\mathbb{H}}'$ is the harmonic part. The symmetry group of $\mathbb{C}$ is the intersection of the symmetry groups of its harmonic and deviatoric parts (Forte and Vianello, 1996). As a result, a cubic symmetry forces $\widetilde{\mathbf{H}}_1' = \gamma_1 \mathbf{I}$ and $\widetilde{\mathbf{H}}_2' = \gamma_2 \mathbf{I}$. From $\mathrm{tr}(\widetilde{\mathbf{H}}_1') = 0$ and $\mathrm{tr}(\widetilde{\mathbf{H}}_2') = 0$ one concludes $\gamma_1 = 0$ and $\gamma_2 = 0$, respectively. Therefore, the tensors $\widetilde{\mathbf{H}}_1'$ and $\widetilde{\mathbf{H}}_2'$ vanish and the harmonic decomposition of the single crystal stiffness reduces to

$$\widetilde{\mathbb{C}} = h_1 \mathbb{P}_1^{\mathrm{I}} + h_2 \mathbb{P}_2^{\mathrm{I}} + \widetilde{\mathbb{H}}'. \tag{30}$$

After averaging Eq. (30) over the orientation space, one obtains for the arithmetic mean

$$\widetilde{\mathbb{C}}^{\mathrm{V}} = h_1 \mathbb{P}_1^{\mathrm{I}} + h_2 \mathbb{P}_2^{\mathrm{I}} + \widetilde{\mathbb{H}}'^{\mathrm{V}}, \quad \widetilde{\mathbb{H}}'^{\mathrm{V}} = \int_g f(g) \widetilde{\mathbb{H}}'(g) \, \mathrm{d}g. \tag{31}$$

Comparing the quantities $h_{1,2}$ and $\widetilde{\mathbb{H}}'^{\mathrm{V}}$ with the first term of Eq. (21), one concludes

$$h_1 = \lambda_1^{\mathrm{VI}}, \quad h_2 = \lambda_2^{\mathrm{VI}}, \quad \widetilde{\mathbb{H}}'^{\mathrm{V}} = \zeta^{\mathrm{V}} \widetilde{\mathbb{A}}'. \tag{32}$$

Analogous results can be obtained for the geometric and the harmonic mean. The following relations hold $3K = \lambda_1^{\mathrm{VI}}$ and $2G = \lambda_2^{\mathrm{VI}}$, where K and G denote the bulk and shear modulus of the isotropic Voigt bound.

4. Flow rule and growth law of the elasticity tensor on the macroscale

4.1. Flow rule on the macroscale

Some of the deformation modes, which describe important metal forming operations, are characterized macroscopically by velocity gradients ($\mathbf{L} = \mathbf{D} + \mathbf{W}$) with a vanishing skew part $\mathbf{W}$. Examples of operations, which are described by the stretching tensor $\mathbf{D}$ alone, are the modes of simple tension, plane strain compression, and simple compression. In the present paper only processes with $\mathbf{W} = \mathbf{0}$ are considered. For this case the evolution of the initially isotropic elastic properties due to a constant $\mathbf{D}$ is investigated. The flow

rule is required to reflect the evolving anisotropy of the stress–strain relation and hence has to be anisotropic, if $\widetilde{\mathbb{A}}' \neq 0$ holds. In order to avoid an interference of different physical effects, hardening phenomena are not included in this paper.

The physical assumption that the elastic behavior within the grains, i.e. on the microscale, is not affected by inelastic deformations results in a rather straightforward approach to plasticity. Instead of determining the path-dependent elastic law $\mathbf{h}$, a constant elastic referential law $\tilde{\mathbf{h}}$ and an evolution equation for the inelastic transformation $\mathbf{P}$ are required. This paper aims to derive a model that describes the evolution of the elastic properties. Therefore, the aforementioned approach to plasticity based on isomorphic elastic ranges is not applicable on the macroscale. A simple extension of this approach is obtained by postulating an evolution equation for the referential elastic law $\tilde{\mathbf{h}}$ while maintaining the formula (3).

In the following the formulation of constitutive equations is based on the assumption of fixed reference functions with respect to the undistorted state. This assumption generalizes the concept of isomorphic material functions (Bertram, 1992, 1999). The following representation of the flow rule with respect to the undistorted state is postulated

$$\mathbf{P}^{-1}\dot{\mathbf{P}} = \widetilde{\mathbf{K}}(\widetilde{\mathbf{C}}, \mathbf{P}^{\mathrm{T}}\dot{\mathbf{C}}\mathbf{P}, \widetilde{\mathbb{A}}'). \tag{33}$$

Equivalent forms of the flow rule can be formulated with respect to the reference and current placement as it was done for the elastic law in Eq. (5)

$$\begin{aligned} \dot{\mathbf{P}}\mathbf{P}^{-1} &= \mathbf{K}(\mathbf{C}, \dot{\mathbf{C}}, \mathbb{A}'), \\ \mathbf{F}\dot{\mathbf{P}}\mathbf{P}^{-1}\mathbf{F}^{-1} &= \mathbf{K}_{\mathrm{E}}(\mathbf{B}, \dot{\mathbf{B}}, \mathbb{A}'_{\mathrm{E}}). \end{aligned} \tag{34}$$

The following transformation rules hold between the different functions

$$\begin{aligned} \mathbf{K}(\mathbf{C}, \dot{\mathbf{C}}, \mathbb{A}') &= \mathbf{P}\widetilde{\mathbf{K}}(\mathbf{P}^{\mathrm{T}}\mathbf{C}\mathbf{P}, \mathbf{P}^{\mathrm{T}}\dot{\mathbf{C}}\mathbf{P}, \mathbf{P}^{-1} \times \mathbb{A}')\mathbf{P}^{-1}, \\ \mathbf{K}_{\mathrm{E}}(\mathbf{B}, \dot{\mathbf{B}}, \mathbb{A}'_{\mathrm{E}}) &= \widetilde{\mathbf{F}}\widetilde{\mathbf{K}}(\widetilde{\mathbf{F}}^{\mathrm{T}}\mathbf{F}^{-1}\mathbf{B}\mathbf{F}^{-\mathrm{T}}\widetilde{\mathbf{F}}, \mathbf{P}^{\mathrm{T}}\mathbf{R}^{\mathrm{T}}\mathscr{L}(\mathbf{B}, \mathbf{R})\mathbf{R}\mathbf{P}, \widetilde{\mathbf{F}}^{-1} \times \widetilde{\mathbb{A}}'_{\mathrm{E}})\widetilde{\mathbf{F}}^{-1}, \end{aligned} \tag{35}$$

where $\mathbf{B}$ denotes the left Cauchy–Green tensor. Similar to Eq. (5), the functions $\mathbf{K}$ and $\mathbf{K}_{\mathrm{E}}$ result from transforming the constant function $\widetilde{\mathbf{K}}$ by the inelastic transformation $\mathbf{P}$ and by the deformation gradient $\mathbf{F}$, respectively. Constraints are given by the incompressibility conditions for inelastic deformations $\det(\mathbf{P}) = 1$, or equivalently $\mathrm{tr}(\mathbf{P}^{-1}\dot{\mathbf{P}}) = 0$. If a rate-independent behavior is to be modeled, the functions (33) and (34) would have to be positive homogeneous of degree one in the rate terms.

As an example for isomorphic material functions in the generalized sense, a widely used flow rule for single crystals is given (see, e.g., Asaro and Needleman, 1985; Harren et al., 1989)

$$\mathbf{P}^{-1}\dot{\mathbf{P}} = -\sum_{\alpha} \dot{\gamma}_{\alpha}(\widetilde{\mathbf{C}})\widetilde{\mathbf{d}}_{\alpha} \otimes \widetilde{\mathbf{n}}^{\alpha}, \quad \dot{\gamma}_{\alpha} = \dot{\gamma}_0 \,\mathrm{sign}(\tau_{\alpha}) \left| \frac{\tau_{\alpha}}{\tau_{\alpha}^{\mathrm{D}}} \right|^{1/m}, \quad \tau_{\alpha} = \widetilde{\mathbf{C}}\widetilde{\mathbf{h}}(\widetilde{\mathbf{C}}) \cdot \widetilde{\mathbf{d}}_{\alpha} \otimes \widetilde{\mathbf{n}}^{\alpha}. \tag{36}$$

Note that $\mathbf{P}^{-1}\dot{\mathbf{P}} = -\dot{\mathbf{F}}_{\mathrm{p}}\mathbf{F}_{\mathrm{p}}^{-1}$ holds. In this case the function $\widetilde{\mathbf{K}}$ depends only on $\widetilde{\mathbf{C}}$ and is specified in terms of Schmid tensors $\widetilde{\mathbf{d}}_{\alpha} \otimes \widetilde{\mathbf{n}}^{\alpha}$ and corresponding shear rates $\dot{\gamma}_{\alpha}$. $\tau_{\alpha}^{\mathrm{D}}$ denotes the drag stress and τ_{α} the resolved shear stress in the slip system α. The parameter m is called the strain rate sensitivity. The Mandel stress tensor $\widetilde{\mathbf{C}}\widetilde{\mathbf{h}}(\widetilde{\mathbf{C}}) = \widetilde{\mathbf{C}}\widetilde{\mathbf{S}}$ can be approximated by $\widetilde{\mathbf{C}}\widetilde{\mathbf{S}} \approx \widetilde{\mathbf{S}}$ in the case of small elastic deformations.

There is experimental evidence that the effective elastic and (visco)plastic properties are correlated for moderately textured polycrystals (Bunge and Roberts, 1969; Stickels and Mould, 1970; Kallend and Davies, 1971; Davies et al., 1972). Therefore, the anisotropy of the (visco)plastic behavior (e.g., the contraction ratio) can be inferred not only from destructive tests but also from non-destructive measurements of the elastic anisotropy parameters. Based on these findings, Man (1995) formulated a quadratic yield function, which is derived from the assumption that the elastic and plastic properties are linearly correlated. As a result, the anisotropic part of the effective elasticity tensor specifies the anisotropic part of the quadratic

yield condition. The introduction of a quadratic yield function goes back to Mises (1928), who introduced a general fourth-order tensor of plastic moduli that establishes an anisotropic quadratic yield condition in terms of stresses. In the following a stress space formulation of the flow rule is preferred. The corresponding strain space description is obtained by replacing the stress tensor $\widetilde{\mathbf{S}}$ by $\tilde{\mathbf{h}}(\widetilde{\mathbf{C}})$. Based on the restriction that only coaxial deformation processes are considered, i.e. $\mathbf{W} = \mathbf{0}$, it is assumed that the skew part $\widetilde{\mathbf{W}}_p = -\text{skw}(\mathbf{P}^{-1}\dot{\mathbf{P}})$ vanishes. This assumption is acceptable since the texture simulations of coaxial processes do not indicate a rotation of the symmetry axes of the effective elasticity tensor.

A simple extension of the viscoplastic flow rule (36) to the macroscale is obtained by introducing an anisotropic norm, which is specified by $\widetilde{\mathbb{A}}'$

$$\|\widetilde{\mathbf{S}}'\|_a = \sqrt{\widetilde{\mathbf{S}}' \cdot \widetilde{\mathbb{N}}[\widetilde{\mathbf{S}}']}, \quad \widetilde{\mathbb{N}} = \mathbb{P}_2^I + \eta \widetilde{\mathbb{A}}'. \tag{37}$$

The condition $\eta \in (-1, 1)$ represents a sufficient (but not necessary) condition for

$$\|\widetilde{\mathbf{S}}'\|_a > 0, \quad \forall \widetilde{\mathbf{S}}' \neq \mathbf{0} \in \text{Sym}. \tag{38}$$

This estimate is based upon the property $\|\widetilde{\mathbb{A}}'\| \in [0, 1]$ of the tensor $\widetilde{\mathbb{A}}'$, and the inequality

$$-\|\widetilde{\mathbb{A}}'\| \leqslant \widetilde{\mathbf{S}}'^* \cdot \widetilde{\mathbb{A}}'[\widetilde{\mathbf{S}}'^*] \leqslant +\|\widetilde{\mathbb{A}}'\|, \tag{39}$$

which holds for all $\widetilde{\mathbf{S}}'^* = \widetilde{\mathbf{S}}'/\|\widetilde{\mathbf{S}}'\|$.

An anisotropic flow rule based on the aforementioned quadratic form is given by

$$\widetilde{\mathbf{D}}'_p = \frac{\dot{\gamma}_0}{\|\widetilde{\mathbf{S}}'\|_a} \left(\frac{\sqrt{\frac{3}{2}}\|\widetilde{\mathbf{S}}'\|_a}{\sigma_D} \right)^{1/m} \widetilde{\mathbb{N}}[\widetilde{\mathbf{S}}'], \quad \widetilde{\mathbf{D}}'_p = -\text{sym}(\mathbf{P}^{-1}\dot{\mathbf{P}}). \tag{40}$$

$\widetilde{\mathbf{D}}'_p$ denotes the symmetric part of the inelastic rate of deformation with respect to the undistorted state. An isotropic (J_2-type) flow rule results for both $\eta = 0$ and $\widetilde{\mathbb{A}}' = \mathbb{O}$.

4.2. Growth law for the elasticity tensor on the macroscale

The function $\tilde{\mathbf{h}}$ has been linearized in the present paper, and the micro-mechanical considerations motivate an additive split of the operator $\widetilde{\mathbb{C}}$ into an isotropic and an anisotropic part

$$\widetilde{\mathbb{C}} = \widetilde{\mathbb{C}}^I + \zeta \widetilde{\mathbb{A}}', \qquad \widetilde{\mathbb{C}}^I = 3K\mathbb{P}_1^I + 2G\mathbb{P}_2^I. \tag{41}$$

K is the bulk modulus and G is the shear modulus for a uniform orientation distribution. If orientation averages are applied, then K and G are independent of the texture of the aggregate and can be estimated by, e.g., Eq. (19). ζ is a scalar parameter and can be estimated by Eq. (22). A property which is peculiar to aggregates of cubic crystals, is that the anisotropic part $\widetilde{\mathbb{A}}'$ is irreducible. In order to predict the evolution of Hooke's law, the rate of change of the tensor $\widetilde{\mathbb{A}}'$ has to be modeled. The single tensor $\widetilde{\mathbb{A}}'$ covers all possible cases of material symmetries that can be induced by a texture in an aggregate of cubic crystals like, e.g., a triclinic behavior, orthotropy, or isotropy. This description of anisotropy differs from the method based on second-order structure tensors (Boehler, 1987), where the number of structure tensors depends on the specific symmetry to be modeled.

Changes of the effective elastic behavior due to an evolving texture are caused by inelastic deformations. Therefore it seems to be natural to assume that the rate of change of the tensor $\widetilde{\mathbb{A}}'$ is governed by the (generally non-symmetric) inelastic rate and the current state of anisotropy

$$\dot{\widetilde{\mathbb{A}}}' = \widetilde{\mathbb{K}}(\mathbf{P}^{-1}\dot{\mathbf{P}}, \widetilde{\mathbb{A}}'). \tag{42}$$

Evolution equations with respect to the reference and current placement can be derived from Eq. (42) and are given by

$$\mathscr{L}(\mathbb{A}', \mathbf{P}) = \mathbb{K}(\dot{\mathbf{P}}\mathbf{P}^{-1}, \mathbb{A}'),$$
$$\mathscr{L}(\mathbb{A}'_{\mathrm{E}}, \widetilde{\mathbf{F}}) = \mathbb{K}_{\mathrm{E}}(\mathbf{F}\dot{\mathbf{P}}\mathbf{P}^{-1}\mathbf{F}^{-1}, \mathbb{A}'_{\mathrm{E}}),$$
(43)

where the following transformation rules hold

$$\mathbb{K}(\dot{\mathbf{P}}\mathbf{P}^{-1}, \mathbb{A}') = \mathbf{P} \times \widetilde{\mathbb{K}}(\mathbf{P}^{-1}\dot{\mathbf{P}}\mathbf{P}^{-1}\mathbf{P}, \mathbf{P}^{-1} \times \mathbb{A}'),$$
$$\mathbb{K}_{\mathrm{E}}(\mathbf{F}\dot{\mathbf{P}}\mathbf{P}^{-1}\mathbf{F}^{-1}, \mathbb{A}'_{\mathrm{E}}) = \widetilde{\mathbf{F}} \times \widetilde{\mathbb{K}}(\widetilde{\mathbf{F}}^{-1}\mathbf{F}\dot{\mathbf{P}}\mathbf{P}^{-1}\mathbf{F}^{-1}\widetilde{\mathbf{F}}, \widetilde{\mathbf{F}}^{-1} \times \mathbb{A}'_{\mathrm{E}}).$$
(44)

It is seen that the objective rates in the formulations (43) are Lie derivatives of the Oldroyd-type. This special type of an objective rate occurs due to the geometric properties of $\mathbb{A}'$, i.e. the transformation rule $\mathbb{A}'_{\mathrm{E}} = \widetilde{\mathbf{F}} \times \widetilde{\mathbb{A}}'$, and the constraint $\overset{\triangle}{\widetilde{\mathbb{A}}}{}' = \mathbb{O}$ in the case of constant elastic properties. A strain space formulation of the evolution law is obtained by replacing the inelastic rate term $\mathbf{P}^{-1}\dot{\mathbf{P}}$ in the right-hand sides of Eqs. (42) and (43) by the strain space formulations (33) or (34).

A rigorous simplification is given by the following ansatz for the function $\widetilde{\mathbb{K}}$

$$\widetilde{\mathbb{K}}(\mathbf{P}^{-1}\dot{\mathbf{P}}, \widetilde{\mathbb{A}}') = K_1(\widetilde{\mathbf{D}}'_{\mathrm{p}}, \widetilde{\mathbb{A}}')\mathbb{G}'(\widetilde{\mathbf{D}}'_{\mathrm{p}}) - K_2(\widetilde{\mathbf{D}}'_{\mathrm{p}}, \widetilde{\mathbb{A}}')\widetilde{\mathbb{A}}'.$$
(45)

The growth law (45) is similar to a kinematical hardening model, which was formulated for second-order backstress tensors by Armstrong and Frederick (1966). Krempl (1994) proposed a similar ansatz in the context of fourth-order internal variables. The functions K_1, K_2, and $\mathbb{G}'$ are isotropic in their arguments since the anisotropy is taken explicitly into account by the tensor $\widetilde{\mathbb{A}}'$. The fourth-order tensor function $\mathbb{G}'$ can be determined by means of the theory of isotropic tensor functions. In the following Eq. (45) is further simplified by setting $K_2 = 0$ and assuming that the saturation of $\widetilde{\mathbb{A}}'$ is governed by $K_1 = K$.

The general representation of the tensor function $\mathbb{G}'(\widetilde{\mathbf{D}}'_{\mathrm{p}})$ is derived in the Appendices A and B. In Appendix A the fourth-order isotropic tensor function $\mathbb{G}$ of a symmetric second-order tensor $\widetilde{\mathbf{D}}'_{\mathrm{p}}$ is determined with $\mathbb{G}$ having the major symmetry and the symmetries in the first and second pair of indices. In Appendix B the irreducible part $\mathbb{G}'$ of $\mathbb{G}$ is presented. The constraint of irreducibility simplifies the function $\mathbb{G}$ considerably. The function $\mathbb{G}'$ depends only on three tensor generators and three scalar functions, which are isotropic in the inelastic rate of deformation

$$\mathbb{G}'(\widetilde{\mathbf{D}}'_{\mathrm{p}}) = g_{11}(\widetilde{\mathbf{D}}'_{\mathrm{p}})\mathbb{G}'_3(\widetilde{\mathbf{D}}'_{\mathrm{p}}) + g_{22}(\widetilde{\mathbf{D}}'_{\mathrm{p}})\mathbb{G}'_4(\widetilde{\mathbf{D}}'_{\mathrm{p}}) + g_{12}(\widetilde{\mathbf{D}}'_{\mathrm{p}})\mathbb{G}'_9(\widetilde{\mathbf{D}}'_{\mathrm{p}}).$$
(46)

If the texture evolution is assumed to be rate-independent, then the growth law (42) is homogeneous of degree one in the inelastic rate, which leads to the special form

$$\overset{\triangle}{\widetilde{\mathbb{A}}}{}' = \|\widetilde{\mathbf{D}}'_{\mathrm{p}}\| K(\widetilde{\mathbf{N}}'_{\mathrm{p}}, \widetilde{\mathbb{A}}')(G_3(I_{\mathrm{p}})\mathbb{G}'_3(\widetilde{\mathbf{N}}'_{\mathrm{p}}) + G_4(I_{\mathrm{p}})\mathbb{G}'_4(\widetilde{\mathbf{N}}'_{\mathrm{p}}) + G_9(I_{\mathrm{p}})\mathbb{G}'_9(\widetilde{\mathbf{N}}'_{\mathrm{p}})),$$
(47)

where $\widetilde{\mathbf{N}}'_{\mathrm{p}} = \widetilde{\mathbf{D}}'_{\mathrm{p}}/\|\widetilde{\mathbf{D}}'_{\mathrm{p}}\|$. The functions G_i depend on the only non-vanishing principal invariant of $\widetilde{\mathbf{N}}'_{\mathrm{p}}$

$$G_i(\widetilde{\mathbf{D}}'_{\mathrm{p}}) = G_i(I_{\mathrm{p}}), \quad I_{\mathrm{p}} = \det(\widetilde{\mathbf{N}}'_{\mathrm{p}}).$$
(48)

If the interaction of the inelastic rate of deformation and the elastic anisotropy is negligible with respect to K, then the function K reduces to

$$K(\widetilde{\mathbf{N}}'_{\mathrm{p}}, \widetilde{\mathbb{A}}') = K(I_{\mathrm{p}}, \widetilde{\mathbb{A}}').$$
(49)

There are certain general constraints which have to be considered. As shown before, all solutions $\widetilde{\mathbb{A}}'$ of Eq. (42) have to fulfill $\|\widetilde{\mathbb{A}}'\| \leqslant 1$. In the following it is assumed that the rate of change of $\|\widetilde{\mathbb{A}}'\|$ is

proportional to the difference of the saturation and the current value of $\|\widetilde{\mathbb{A}}'\|$. The saturation value of $\|\widetilde{\mathbb{A}}'\|$ may depend on I_p. The ansatz

$$K(I_p, \widetilde{\mathbb{A}}') = A_\infty(I_p) - \|\widetilde{\mathbb{A}}'\|, \tag{50}$$

ensures the fulfillment of the constraint upon the magnitude of $\widetilde{\mathbb{A}}'$, if the saturation value satisfies the inequality

$$A_\infty(I_p) \leqslant 1, \quad \forall I_p \in \left[-\frac{\sqrt{6}}{18}, +\frac{\sqrt{6}}{18} \right]. \tag{51}$$

Now the growth law is equal to

$$\dot{\widetilde{\mathbb{A}}}' = \|\widetilde{\mathbf{D}}'_p\|(A_\infty(I_p) - \|\widetilde{\mathbb{A}}'\|)(G_3(I_p)\mathbb{G}'_3(\widetilde{\mathbf{N}}'_p) + G_4(I_p)\mathbb{G}'_4(\widetilde{\mathbf{N}}'_p) + G_9(I_p)\mathbb{G}'_9(\widetilde{\mathbf{N}}'_p)). \tag{52}$$

Moreover, the elasticity tensor $\widetilde{\mathbb{C}}$ in Eq. (41) has to be positive definite for all solutions $\widetilde{\mathbb{A}}'$ of Eq. (42). In the following, a sufficient condition is formulated. For aggregates of cubic crystals the (elastic) dilatational and isochoric deformation modes are uncoupled. Furthermore, the eigenvalue of the effective stiffness corresponding to the dilatational mode is equal to that one of the single crystal ($\lambda_1 = \lambda_1^V = \lambda_1^A = \lambda_1^K$). If $\lambda_1 = \widetilde{\mathbb{C}} \cdot \mathbb{P}_1^I > 0$ holds, the condition of positive definiteness of the effective stiffness (41) reduces to

$$0 < \widetilde{\mathbf{E}}'^* \cdot (\widetilde{\mathbb{C}} - \lambda_1 \mathbb{P}_1^I)[\widetilde{\mathbf{E}}'^*], \quad \forall \widetilde{\mathbf{E}}'^* = \frac{\widetilde{\mathbf{E}}'}{\|\widetilde{\mathbf{E}}'\|} \neq \mathbf{0} \in \text{Sym}. \tag{53}$$

Based on the inequality $\widetilde{\mathbf{E}}'^* \cdot \widetilde{\mathbb{A}}'[\widetilde{\mathbf{E}}'^*] \geqslant -\|\widetilde{\mathbb{A}}'\|\forall\widetilde{\mathbf{E}}'^*$, one concludes that as long as

$$\|\widetilde{\mathbb{A}}'\| < \frac{2G}{\zeta} \tag{54}$$

holds, the positive definiteness is guaranteed.

5. Numerical examples

5.1. Parameterization of deformation processes

The stretching tensor can generally be decomposed as

$$\mathbf{D} = \|\mathbf{D}\|\mathbf{Q}_D\mathbf{N}_D\mathbf{Q}_D^T, \tag{55}$$

where $\|\mathbf{D}\|$ is the magnitude of $\mathbf{D}$, and $\mathbf{Q}_D$ is an orthogonal tensor that maps an arbitrary reference basis $\{\mathbf{e}_i\}$ onto the eigenvectors of $\mathbf{D}$. The eigenvectors of the symmetric tensor $\mathbf{N}_D$ are $\{\mathbf{e}_i\}$, and the eigenvalues n_α of $\mathbf{N}_D$ are equal to those of $\mathbf{D}$ divided by $\|\mathbf{D}\|$. The restriction $\text{tr}(\mathbf{D}) = 0$ can be imposed on $\mathbf{D}$ because the considered inelastic deformations are isochoric. As a result, the eigenvalues n_α are constrained by $n_1 + n_2 + n_3 = 0$ and $n_1^2 + n_2^2 + n_3^2 = 1$. These constraints are identically fulfilled by the following parameterization of $\mathbf{N}_D$

$$\mathbf{N}_D = \sum_{\alpha=1}^3 n_\alpha \mathbf{e}_\alpha \otimes \mathbf{e}_\alpha, \quad n_{1,3} = -\frac{\sqrt{6}}{6}\xi \pm \frac{\sqrt{2}}{2}\sqrt{1-\xi^2}, \quad n_2 = \frac{\sqrt{6}}{3}\xi, \tag{56}$$

$\xi \in [-0.5, +0.5]$. This range of ξ is sufficient to describe all $\mathbf{D}$. The principal invariants of $\mathbf{D}$ are

$$I_1 = 0, \quad I_2 = -\frac{1}{2}\|\mathbf{D}\|^2, \quad I_3 = \frac{\sqrt{6}}{6}\|\mathbf{D}\|^3 \xi\left(\frac{4}{3}\xi^2 - 1\right). \tag{57}$$

It can be concluded that the geometrical type of the deformation is only influenced by the third principal invariant, i.e. the determinant, of the **D**. The ξ-values -0.5, 0, and $+0.5$ belong to uniaxial elongation, plane strain compression, and simple compression, respectively.

5.2. Texture simulation based on the Taylor–Lin model

Here the Taylor–Lin model (Taylor, 1938; Lin, 1957) is applied, which allows for elastic deformations of the crystal lattices. Similar to Taylor's original approach, the Taylor–Lin model treats compatibility constraints as paramount and assumes the deformation of the aggregate to be homogeneous. The crystallographic texture evolution of metals with high or intermediate stacking fault energy can be determined by Taylor-type models within a first-order accuracy (Harren and Asaro, 1989; Leffers, 1993). There is still a discussion why Taylor-type models are able to model pure metal textures, but fail to reproduce alloy textures (see, e.g., Kocks et al., 1998, p. 413).

Plastic deformations in single crystals are dominated by slip mechanisms on specific crystallographic planes. In the case of copper at room temperature, the slip on the octahedral slip systems $\{1\,1\,1\}\langle1\,1\,0\rangle$ is of prime importance. In the present paper we adopt a rate-dependent model as given by Eq. (36) (Asaro and Needleman, 1985; Wu et al., 1996). The material functions and parameters for the single crystal stiffness and the flow rule are given in Tables 1 and 2. The simulations are performed with 1000 modified random orientations (Böhlke and Bertram, 1998).

The Taylor–Lin model is used for the determination of the evolution of $\mathbb{A}'_E = \widetilde{\mathbf{F}} \times \widetilde{\mathbb{A}}'$ corresponding to macroscopic strain rates with $\xi \in [-0.5, +0.5]$ (see Eq. (56)) and $\mathbf{Q}_D = \mathbf{I}$. As mentioned before, this range of ξ allows the description of all geometrical distinct deformation modes. The specification $\mathbf{Q}_D = \mathbf{I}$ represents no loss of generality since the initial effective stiffness is assumed to be isotropic. The $\mathbb{A}'_E$ is defined analogously to $\widetilde{\mathbb{A}}'$ in terms of Eulerian lattice vectors.

Table 1
Material functions on the microscale

Elastic law	$\mathbf{S} = \mathbf{P}\widetilde{\mathbb{C}}[\frac{1}{2}(\mathbf{P}^T\mathbf{C}\mathbf{P} - \mathbf{I})]\mathbf{P}^T$	(3)
Stiffness tensor	$\widetilde{\mathbb{C}} = 3K\mathbb{P}_1^I + 2G\mathbb{P}_2^I + \zeta\frac{\sqrt{30}}{30}\left(\mathbf{I}\otimes\mathbf{I} + 2\mathbb{I} - 5\sum_{i=1}^{3}\widetilde{\mathbf{g}}_i\otimes\widetilde{\mathbf{g}}_i\otimes\widetilde{\mathbf{g}}_i\otimes\widetilde{\mathbf{g}}_i\right)$	(21)
Flow rule	$\dot{\mathbf{F}}_p\mathbf{F}_p^{-1} = \sum_\alpha \dot{\gamma}_\alpha \widetilde{\mathbf{d}}_\alpha \otimes \widetilde{\mathbf{n}}^\alpha$	(36)
Kinetic equation	$\dot{\gamma}_\alpha = \dot{\gamma}_0 \,\text{sign}(\tau_\alpha)\left\|\frac{\tau_\alpha}{\tau_\alpha^D}\right\|^{\frac{1}{m}}$	(36)

Table 2
Material parameters on the microscale

K (GPa)	G (GPa)	ζ (GPa)	$\dot{\gamma}_0$ (s^{-1})	τ_α^D ($\alpha = 1\dots12$) (MPa)	m
136.93	54.56	114.14	0.001	16	0.0125

5.3. Identification of the phenomenological model

The initial value of the stiffness $\widetilde{\mathbb{C}}$ is assumed to be isotropic. For comparisons of the phenomenological model with the predictions of the Taylor–Lin model the initial value $\widetilde{\mathbb{C}}^{\mathrm{I}}$ is specified by the eigenvalues $3K = \lambda_1^{\mathrm{VI}}$, and $2G = \lambda_2^{\mathrm{VI}}$. The scalar ζ is equal to ζ^{V}. Based on Eq. (54) one concludes that the positive definiteness of the effective stiffness tensor is ensured as long as $\|\widetilde{\mathbb{A}}'\| \leqslant 0.96$ holds. The simulations show that this inequality is fulfilled for all considered rate of deformations.

For comparisons of the phenomenological model with experiments, the tensor $\mathbb{C}^{\mathrm{I}}$ is determined by the eigenvalues $3K = \lambda_1^{\mathrm{VI}}$, and $2G = 0.85\lambda_2^{\mathrm{VI}}$. The scalar ζ is equal to $0.6\zeta^{\mathrm{V}}$. As a result, the positive definiteness is generally fulfilled, since $2G/\zeta = 1.35 > 1$ holds (see Eq. (54)).

The flow rule of the polycrystal is assumed to be governed by Eq. (40). The reference shear rate and the strain rate sensitivity are equal to the microscopic values. The constant η controls the coupling between the elastic and (visco)plastic anisotropy. Here the maximum magnitude of η in the sense of the above mentioned constraint $\eta \in (-1, +1)$ is used.

For the evolution equation of the tensor $\widetilde{\mathbb{A}}'$ the functions $A_\infty(I_{\mathrm{p}})$ and $G_\alpha(I_{\mathrm{p}})$ are needed. The micro–macro simulations deliver estimates for the saturation values A_∞ vs ξ (Table 3). A difficult problem is the determination of the functions $G_i(I_{\mathrm{p}})$, which specify the direction of $\dot{\widetilde{\mathbb{A}}}'$ in terms of the direction of the inelastic rate of deformation. Here again, the texture simulations indicate the way. Inspection of these simulations shows that certain components of $\widetilde{\mathbb{A}}'$ do not evolve for certain ξ-values. In the case of a plane strain compression deformation, i.e. $\xi = 0$, with $\mathbf{e}_1$ and $\mathbf{e}_3$ the rolling and normal direction, respectively, $\widetilde{A}_{2233} = \widetilde{A}_{3333} = 0$ holds. If the inelastic rate of deformation is set to be equal to macroscopic rate of deformation, i.e. $\mathbf{N}'_{\mathrm{p}} = (\mathbf{e}_1 \otimes \mathbf{e}_1 - \mathbf{e}_3 \otimes \mathbf{e}_3)/\sqrt{2}$, Eq. (52) implies

$$G_3 = \frac{\sqrt{2}}{14} G_9, \quad G_4 = \frac{17\sqrt{2}}{7} G_9. \tag{58}$$

Similar considerations give the numerical values of $G_i(I_{\mathrm{p}})$ (Table 3). The material functions and parameters which have been used for the macrosimulation are summarized in Tables 4 and 5. If two parameters are given then the first is used for comparisons with the Taylor–Lin model whereas the second one specifies the model, which is compared with experimental data.

5.4. Comparison of the predictions of the Taylor–Lin and the phenomenological model

Plane strain compression. The channel-die test is well suited for measuring the material response under monotonic deformation. The textures produced by this deformation are generally more reliable than those determined from ill-controlled rolling experiments. Fig. 2 (left) shows the components of $\mathbb{C}_{\mathrm{E}} = \widetilde{\mathbf{F}} \times \widetilde{\mathbb{C}}$ as predicted by both the texture simulation and the phenomenological model. The components are plotted vs the equivalent strain $\phi = \sqrt{2/3} \int \|\mathbf{D}\| \, \mathrm{d}t$. The stiffness $\mathbb{C}_{\mathrm{E}}$ is determined as a volume average of the Eulerian stiffness tensors of the single crystals forming the aggregate. The corresponding matrices are presented in

Table 3
Functions A_∞ and G_i vs ξ

ξ	$-\frac{1}{2}$	$-\frac{1}{4}$	0	$\frac{1}{4}$	$\frac{1}{2}$
A_∞	0.192	0.302	0.500	0.350	0.200
$G_3/G_3(0)$	1.400	1.120	1.000	−2.000	−3.970
$G_4/G_4(0)$	1.400	1.120	1.000	1.000	−3.970
$G_9/G_9(0)$	1.400	1.120	1.000	1.000	−3.970
	$G_3(0) = 0.075$		$G_4(0) = 2.570$		$G_9(0) = 0.750$

Table 4
Material functions on the macroscale

Elastic law	$\mathbf{S} = \mathbf{P}\widetilde{\mathbb{C}}[\frac{1}{2}(\mathbf{P}^{\mathrm{T}}\mathbf{C}\mathbf{P} - \mathbf{I})]\mathbf{P}^{\mathrm{T}}$	(3)
Stiffness tensor	$\widetilde{\mathbb{C}} = 3K\mathbb{P}_1^{\mathrm{I}} + 2G\mathbb{P}_2^{\mathrm{I}} + \zeta\widetilde{\mathbb{A}}'$	(21)
Interpretation	$\widetilde{\mathbb{A}}' = \dfrac{\sqrt{30}}{30}\left(\mathbf{I}\otimes\mathbf{I} + 2\mathbb{I} - 5\displaystyle\int_g\sum_{k=1}^{3}f(g)\widetilde{\mathbf{g}}_k\otimes\widetilde{\mathbf{g}}_k\otimes\widetilde{\mathbf{g}}_k\otimes\widetilde{\mathbf{g}}_k\,\mathrm{d}g\right)$	(25)
Properties	$\widetilde{A}'_{ijkl} = \widetilde{A}'_{jikl} = \widetilde{A}'_{klij} = \widetilde{A}'_{kjil} = \cdots, \qquad A'_{iikl} = 0$	(27)
Flow rule	$\widetilde{\mathbf{D}}'_{\mathrm{p}} = \dfrac{\dot{\gamma}_0}{\|\widetilde{\mathbf{S}}'\|_a}\left(\dfrac{\sqrt{\frac{3}{2}}\|\widetilde{\mathbf{S}}'\|_a}{\sigma_{\mathrm{D}}}\right)^{\frac{1}{m}}\widetilde{\mathbb{N}}[\widetilde{\mathbf{S}}'] \qquad \widetilde{\mathbf{D}}'_{\mathrm{p}} = \mathrm{sym}(\dot{\mathbf{F}}_{\mathrm{p}}\mathbf{F}_{\mathrm{p}}^{-1})$	(40)
Inelastic compliance	$\widetilde{\mathbb{N}} = \mathbb{P}_2^{\mathrm{I}} + \eta\widetilde{\mathbb{A}}'$	(40)
Anisotropic norm	$\|\widetilde{\mathbf{S}}'\|_a = \sqrt{\widetilde{\mathbf{S}}'\cdot\widetilde{\mathbb{N}}[\widetilde{\mathbf{S}}']}$	(37)
Growth law	$\dot{\widetilde{\mathbb{A}}}' = \|\widetilde{\mathbf{D}}'_{\mathrm{p}}\|K(\widetilde{\mathbf{N}}'_{\mathrm{p}}, \widetilde{\mathbb{A}}')\mathbb{G}'(\widetilde{\mathbf{N}}'_{\mathrm{p}})$	(47)
	$\widetilde{\mathbf{N}}'_{\mathrm{p}} = \widetilde{\mathbf{D}}'_{\mathrm{p}}/\|\widetilde{\mathbf{D}}'_{\mathrm{p}}\| \quad I_{\mathrm{p}} = \det(\widetilde{\mathbf{N}}'_{\mathrm{p}})$	
Scalar valued function	$K(\widetilde{\mathbf{N}}'_{\mathrm{p}}, \widetilde{\mathbb{A}}') = A_\infty(I_{\mathrm{p}}) - \|\widetilde{\mathbb{A}}'\|$	(50)
Tensor valued function	$\mathbb{G}'(\widetilde{\mathbf{N}}'_{\mathrm{p}}) = G_3(I_{\mathrm{p}})\mathbb{G}'_3(\widetilde{\mathbf{N}}'_{\mathrm{p}}) + G_4(I_{\mathrm{p}})\mathbb{G}'_4(\widetilde{\mathbf{N}}'_{\mathrm{p}}) + G_9(I_{\mathrm{p}})\mathbb{G}'_9(\widetilde{\mathbf{N}}'_{\mathrm{p}})$	(46)

Table 5
Material parameters on the macroscale

K (GPa)	G (GPa)	ζ (GPa)	σ_{D} (MPa)	$\dot{\gamma}_0$ (s^{-1})	m	η
136.93	54.56/46.37	114.14/68.49	46.5	0.001	0.0125	0.999

Appendix C. A discriminating test is given by a comparison of the eigenvalues of the effective stiffness tensor. In Fig. 2 (right) the eigenvalues are shown except the one with respect to the dilatational deformation mode, which is not affected by the evolving texture. The numerical results indicate that there is no saturation of the amount of elastic anisotropy even for equivalent strains of $\phi \approx 2.7$. The amount of anisotropy is then given by $\|\mathbb{A}'_{\mathrm{E}}\| \approx 0.37$. Note that for a single crystal $\|\mathbb{A}'_{\mathrm{E}}\|$ is equal to one.

In Fig. 3 the predictions of the phenomenological model are compared with experimental values of Young's modulus documented by Weerts (1933) and Alers and Liu (1967). Young's modulus has been measured in the sheet plane of cold-rolled copper. The thickness reduction reaches 96% and 95%, respectively. The parameter θ denotes the angle between the rolling and tensile the direction. In Table 6 the experimental values are compared with the numerical values. The measured values are not bounded by the arithmetic and the harmonic mean because of the overestimated sharpness of the texture given by the Taylor–Lin model.
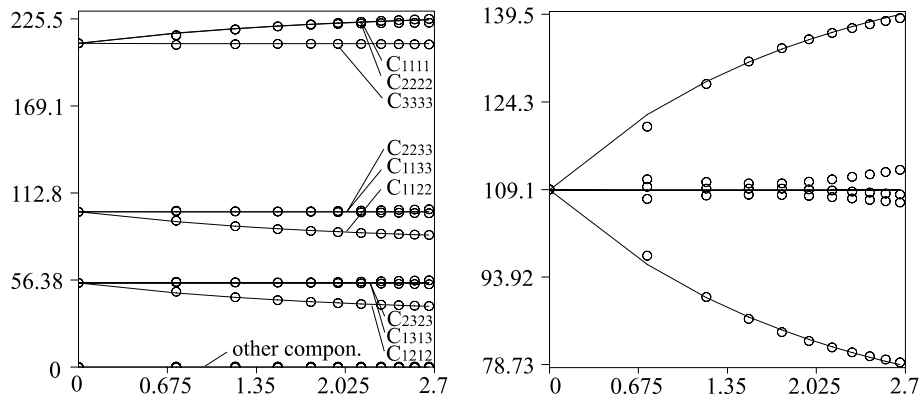
Fig. 2. Components (left) and eigenvalues (right) of the Eulerian stiffness $\mathbb{C}_E$ (GPa) for plane strain compression vs equivalent strain ϕ: (–) phenomenological model, (○) Taylor–Lin model.
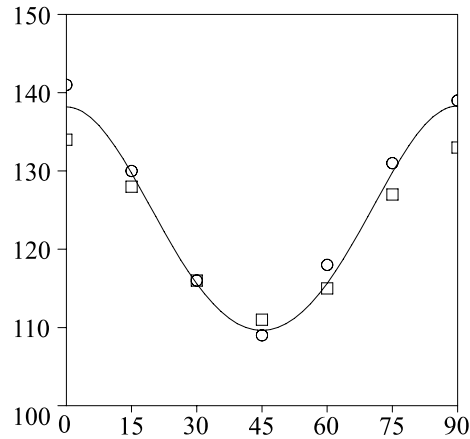

Fig. 3. Predictions of Young's modulus (GPa) vs angle from rolling direction (degrees): (−) phenomenological model, (○) Weerts (1933) (□) Alers and Liu (1967).

Table 6
Young's modulus (GPa) of rolled copper: models vs experiments

θ	0° (RD)	15°	30°	45°	60°	75°	90° (TD)
E^V (Taylor–Lin)	170.21	151.92	125.33	114.95	124.11	148.75	165.46
E^A (Taylor–Lin)	156.43	137.81	111.55	101.51	110.18	134.14	150.80
E^R (Taylor–Lin)	144.27	124.38	97.677	87.82	96.10	119.92	137.19
E (phenomenological model)	140.24	130.49	114.54	107.94	114.50	130.39	140.11
E (Weerts, 1933)	139	131	118	109	116	130	141
E (Alers and Liu, 1967)	133	127	115	111	116	128	134

Simple tension and simple compression. The uniaxial tension test is the most reliable test for the determination of plastic properties. It is the preferred test for the determination of the yield strength and the
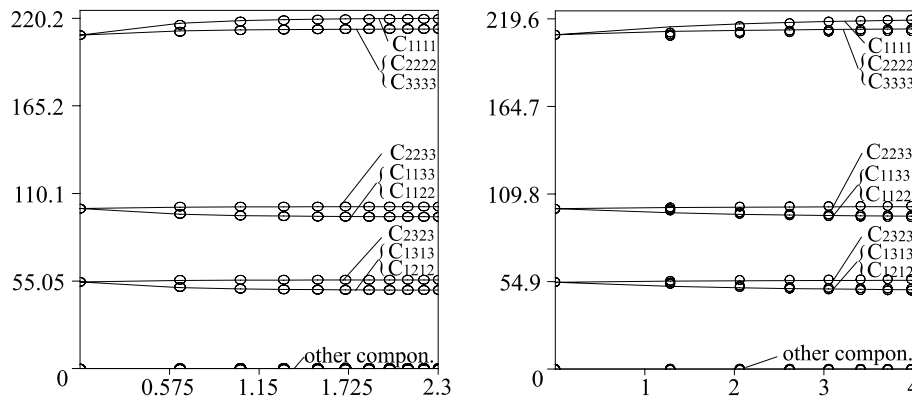
Fig. 4. Components of the Eulerian stiffness $\mathbb{C}_E$ (GPa) vs equivalent strain ϕ for simple tension (left) and simple compression (right); (–) phenomenological model; (○) Taylor–Lin model.

initial strain hardening behavior. For initially non-textured aggregates, such a deformation induces an axisymmetric texture. In Fig. 4 (left) the 21 components of the Eulerian stiffness $\mathbb{C}_E$ are shown. In the case of uniaxial tension, the components of $\mathbb{A}'_E$ are approximately constant for equivalent strain values ϕ larger than 2. The maximum amount of anisotropy is given by $\|\mathbb{A}'_E\| \approx 0.2$.

In the case of the simple compression deformation there is no saturation of the amount of elastic anisotropy even for equivalent strains of $\phi \approx 4$ (see Fig. 4, right). The amount of anisotropy is then given by $\|\mathbb{A}'_E\| \approx 0.18$. It is seen that the phenomenological model is able to predict the texture induced anisotropy as it is given by the Taylor–Lin model.

6. Concluding remarks

In this paper, a phenomenological model has been developed, which describes the evolution of the elastic properties of aggregates of cubic crystals due to a crystallographic texture development. Only deformation processes are considered which can be described by a symmetric velocity gradient. The following main assumptions have been adopted: (i) The elastic anisotropy of the polycrystal can be estimated by orientation averages of the local elasticity tensors. As a result, the elastic anisotropy of cubic crystal aggregates depends on an irreducible fourth-order tensor, which has nine independent components. (ii) The anisotropy of the flow rule is governed by the anisotropy of the elastic behavior. (iii) The direction of the rate of change of the effective elasticity tensor depends on the direction of the inelastic rate of deformation.

The transition from an elastically isotropic initial state to a path dependent final anisotropic state is discussed for the case of polycrystalline copper. The comparison of the suggested model to both micro–macro simulations based on the Taylor–Lin model and to experimental data indicate that the phenomenological model captures the gross features of evolving elasticity tensors.

A continuation of this work should intend to generalize the model to deformation processes that are described by generally non-symmetric macroscopic velocity gradients. In this case the flow rule has to be generally non-symmetric and the evolution of the anisotropic part of the elasticity tensors depends on the plastic spin. As a result, the representation theorem which specifies the growth law of the elasticity tensor has to be extended. Furthermore, the model should be formulated in a thermomechanical framework in order to complete the developed approach.

Appendix A. Fourth-order isotropic tensor function of a symmetric second-order tensor

In the following, we sketch the derivation of the representation of a fourth-order isotropic tensor function $\mathbb{G}$ of a symmetric second-order tensor $\mathbf{A}$. This tensor function is furthermore required to exhibit the index symmetries of elasticity tensors, i.e. the major symmetry and the symmetry in the first and second pair of indices. The starting point is the well-known representation of a (symmetric) second-order isotropic tensor function of two symmetric second-order tensors (Boehler, 1987)

$$\mathbf{G}(\mathbf{A}, \mathbf{B}) = \sum_{\alpha=0}^{7} g_\alpha \mathbf{G}_\alpha. \tag{A.1}$$

The eight isotropic symmetric tensor invariants $\mathbf{G}_\alpha$ are given by

$$\mathbf{I}, \mathbf{A}, \mathbf{A}^2, \mathbf{B}, \mathbf{AB} + \mathbf{BA}, \mathbf{A}^2\mathbf{B} + \mathbf{BA}^2, \mathbf{B}^2, \mathbf{AB}^2 + \mathbf{B}^2\mathbf{A}. \tag{A.2}$$

The g_α are functions of the ten isotropic scalar invariants

$$\mathrm{tr}(\mathbf{A}), \mathrm{tr}(\mathbf{A}^2), \mathrm{tr}(\mathbf{A}^3), \mathrm{tr}(\mathbf{B}), \mathrm{tr}(\mathbf{B}^2), \mathrm{tr}(\mathbf{B}^3), \mathrm{tr}(\mathbf{AB}), \mathrm{tr}(\mathbf{A}^2\mathbf{B}), \mathrm{tr}(\mathbf{AB}^2), \mathrm{tr}(\mathbf{A}^2\mathbf{B}^2). \tag{A.3}$$

The function $\mathbb{G}$ can be obtained by a linearization of $\mathbf{G}$ in $\mathbf{B}$

$$\mathbf{G}^{\mathrm{lin}}(\mathbf{A}, \mathbf{B}) = \mathbb{G}(\mathbf{A})[\mathbf{B}]. \tag{A.4}$$

The linearized function $\mathbf{G}^{\mathrm{lin}}$ is

$$\mathbf{G}^{\mathrm{lin}}(\mathbf{A}, \mathbf{B}) = g_0\mathbf{I} + g_1\mathbf{A} + g_2\mathbf{A}^2 + g_3\mathbf{B} + g_4(\mathbf{AB} + \mathbf{BA}) + g_5(\mathbf{A}^2\mathbf{B} + \mathbf{BA}^2). \tag{A.5}$$

After the linearization, the scalar functions $g_\alpha(\mathbf{A}, \mathbf{B})$ can be expressed in terms of $\mathbf{B}$ and the new functions $g_{ij}(\mathbf{A})$ which are isotropic in $\mathbf{A}$

$$\begin{aligned} g_i &= g_{i0}(\mathbf{A})\mathrm{tr}(\mathbf{B}) + g_{i1}(\mathbf{A})\mathrm{tr}(\mathbf{AB}) + g_{i2}(\mathbf{A})\mathrm{tr}(\mathbf{A}^2\mathbf{B}), &(i = 0, 1, 2), \\ g_i &= g_{i0}(\mathbf{A}), &(i = 3, 4, 5). \end{aligned} \tag{A.6}$$

From the requirement of a major symmetry one concludes

$$g_{10} = g_{01}, \quad g_{20} = g_{02}, \quad g_{12} = g_{21}. \tag{A.7}$$

As a result, the fourth-order isotropic tensor function $\mathbb{G}$ is

$$\begin{aligned} \mathbb{G}(\mathbf{A}) &= \sum_{\alpha=1}^{9} G_\alpha(\mathbf{A})\mathbb{G}_\alpha(\mathbf{A}) \\ &= (3g_{00} + g_{30})\mathbb{P}_1^{\mathrm{I}} + g_{30}\mathbb{P}_2^{\mathrm{I}} + g_{11}\mathbf{A} \otimes \mathbf{A} + g_{22}\mathbf{A}^2 \otimes \mathbf{A}^2 + 2g_{40}\mathbb{J}[\mathbf{A}] + 2g_{50}\mathbb{J}[\mathbf{A}^2] + g_{10}(\mathbf{A} \otimes \mathbf{I} \\ &\quad + \mathbf{I} \otimes \mathbf{A}) + g_{20}(\mathbf{A}^2 \otimes \mathbf{I} + \mathbf{I} \otimes \mathbf{A}^2) + g_{21}(\mathbf{A}^2 \otimes \mathbf{A} + \mathbf{A} \otimes \mathbf{A}^2), \end{aligned} \tag{A.8}$$

where $\mathbb{J}$ is defined by

$$\mathbb{J} = \tfrac{1}{8}(\mathbf{e}_i \otimes \mathbf{e}_j + \mathbf{e}_j \otimes \mathbf{e}_i) \otimes (\mathbf{e}_j \otimes \mathbf{e}_k + \mathbf{e}_k \otimes \mathbf{e}_j) \otimes (\mathbf{e}_k \otimes \mathbf{e}_i + \mathbf{e}_i \otimes \mathbf{e}_k). \tag{A.9}$$

The following relation holds

$$4\mathbb{J}[\mathbf{A}] = (A_{im}\delta_{jn} + A_{in}\delta_{jm} + \delta_{im}A_{jn} + \delta_{in}A_{jm})\mathbf{e}_i \otimes \mathbf{e}_j \otimes \mathbf{e}_m \otimes \mathbf{e}_n. \tag{A.10}$$

Appendix B. Irreducible part of the fourth-order isotropic tensor function of a symmetric second-order tensor

In this appendix we present the irreducible part $\mathbb{G}'$ of the function $\mathbb{G}$ (see Appendix A) by employing the procedure suggested by Cowin (1989). As mentioned before, an irreducible fourth-order tensor is symmetric

and traceless with respect to every pair of indices. Inspection of Eq. (A.8) shows that only the following three of the fourth-order tensor generators in Eq. (A.8) contain non-vanishing irreducible parts

$$\mathbb{G}_3(\mathbf{A}) = \mathbf{A} \otimes \mathbf{A}, \quad \mathbb{G}_4(\mathbf{A}) = \mathbf{A}^2 \otimes \mathbf{A}^2, \quad \mathbb{G}_9(\mathbf{A}) = \mathbf{A}^2 \otimes \mathbf{A} + \mathbf{A} \otimes \mathbf{A}^2, \tag{B.1}$$

which are given by

$$\mathbb{G}_3'(\mathbf{A}) = \langle \mathbf{A} \otimes \mathbf{A} \rangle - \tfrac{2}{7}(\text{tr}(\mathbf{A})\langle \mathbf{A} \otimes \mathbf{I} \rangle + 2\langle \mathbf{A}^2 \otimes \mathbf{I} \rangle) + \tfrac{1}{35}(\text{tr}(\mathbf{A}^2) + 2\text{tr}(\mathbf{A}^2))\langle \mathbf{I} \otimes \mathbf{I} \rangle,$$

$$\mathbb{G}_4'(\mathbf{A}) = \mathbb{G}_3'(\mathbf{A}^2),$$

$$\mathbb{G}_9'(\mathbf{A}) = \langle \mathbf{A}^2 \otimes \mathbf{A} \rangle - \tfrac{2}{7}(\text{tr}(\mathbf{A}^2)\langle \mathbf{A} \otimes \mathbf{I} \rangle + \text{tr}(\mathbf{A})\langle \mathbf{A}^2 \otimes \mathbf{I} \rangle + 4\langle \mathbf{A}^3 \otimes \mathbf{I} \rangle)$$
$$\qquad + \tfrac{2}{35}(\text{tr}(\mathbf{A})\text{tr}(\mathbf{A}^2) + 2\text{tr}(\mathbf{A}^3))\langle \mathbf{I} \otimes \mathbf{I} \rangle. \tag{B.2}$$

The bracket formula $\langle \cdot \rangle$ is defined by $(\mathbf{A}, \mathbf{B} \in \text{Sym})$

$$\langle A_{ij}B_{kl} \rangle = \tfrac{1}{6}(A_{ij}B_{kl} + A_{ik}B_{jl} + A_{il}B_{kj} + B_{ij}A_{kl} + B_{ik}A_{jl} + B_{il}A_{kj}) \tag{B.3}$$

and represents the sum of all possible different permutations of $A_{ij}B_{kl}$ divided by six. Hence, $\mathbb{G}'$ is given by

$$\mathbb{G}'(\mathbf{A}) = g_{11}\mathbb{G}_3'(\mathbf{A}) + g_{22}\mathbb{G}_4'(\mathbf{A}) + g_{12}\mathbb{G}_9'(\mathbf{A}). \tag{B.4}$$

If the tensor $\mathbf{A}$ is replaced by the direction of its deviatoric part $\mathbf{N}'$, then the generators are

$$\mathbb{G}_3'(\mathbf{N}') = \langle \mathbf{N}' \otimes \mathbf{N}' \rangle - \tfrac{4}{7}\langle \mathbf{N}'^2 \otimes \mathbf{I} \rangle + \tfrac{2}{35}\text{tr}(\mathbf{N}'^2)\langle \mathbf{I} \otimes \mathbf{I} \rangle,$$

$$\mathbb{G}_4'(\mathbf{N}') = \langle \mathbf{N}'^2 \otimes \mathbf{N}'^2 \rangle - \tfrac{2}{7}(\text{tr}(\mathbf{N}'^2)\langle \mathbf{N}'^2 \otimes \mathbf{I} \rangle + 2\langle \mathbf{N}'^4 \otimes \mathbf{I} \rangle) + \tfrac{1}{35}(\text{tr}(\mathbf{N}'^2)^2 + 2\text{tr}(\mathbf{N}'^4))\langle \mathbf{I} \otimes \mathbf{I} \rangle, \tag{B.5}$$

$$\mathbb{G}_9'(\mathbf{N}') = \langle \mathbf{N}'^2 \otimes \mathbf{N}' \rangle - \tfrac{2}{7}(\text{tr}(\mathbf{N}'^2)\langle \mathbf{N}' \otimes \mathbf{I} \rangle + 4\langle \mathbf{N}'^3 \otimes \mathbf{I} \rangle) + \tfrac{4}{35}\text{tr}(\mathbf{N}'^3)\langle \mathbf{I} \otimes \mathbf{I} \rangle.$$

Appendix C. Young's modulus: comparison of the phenomenological model with the Taylor–Lin model

In the following the effective stiffnesses predicted by the phenomenological model are compared with those given by the Taylor–Lin model. The texture data are used to determine the arithmetic mean. The components of the stiffness tensors refer to an orthonormal basis $\mathbf{B}_\alpha$ of symmetric second-order tensors (Federov, 1968; Cowin, 1990)

$$\mathbf{B}_1 = \mathbf{e}_1 \otimes \mathbf{e}_1, \quad \mathbf{B}_4 = \tfrac{\sqrt{2}}{2}(\mathbf{e}_2 \otimes \mathbf{e}_3 + \mathbf{e}_3 \otimes \mathbf{e}_2),$$

$$\mathbf{B}_2 = \mathbf{e}_2 \otimes \mathbf{e}_2, \quad \mathbf{B}_5 = \tfrac{\sqrt{2}}{2}(\mathbf{e}_1 \otimes \mathbf{e}_3 + \mathbf{e}_3 \otimes \mathbf{e}_1), \tag{C.1}$$

$$\mathbf{B}_3 = \mathbf{e}_3 \otimes \mathbf{e}_3, \quad \mathbf{B}_6 = \tfrac{\sqrt{2}}{2}(\mathbf{e}_1 \otimes \mathbf{e}_2 + \mathbf{e}_2 \otimes \mathbf{e}_1).$$

Note that with respect to this basis, e.g., the C_{44} component is equal to $2C_{2323}$ which differs from the Voigt notation by the factor of 2.

Initial stiffness:

$$\mathbb{C}_E = \begin{bmatrix} 209.660 & 100.620 & 100.620 & 0 & 0 & 0 \\ & 209.660 & 100.620 & 0 & 0 & 0 \\ & & 209.660 & 0 & 0 & 0 \\ & & & 109.040 & 0 & 0 \\ & & & & 109.040 & 0 \\ & & & & & 109.040 \end{bmatrix} \text{GPa}\,\mathbf{B}_\alpha \otimes \mathbf{B}_\beta$$

Elongation ($\xi = -0.5$, $\phi = 2.3$, $\mathbf{e}_1$ elongation direction):

$$
\mathbb{C}_E^{\text{Taylor}} =
\begin{bmatrix}
220.202 & 95.482 & 95.482 & 0 & 0 & 0 \\
 & 213.449 & 101.8349 & 0 & 0 & 0 \\
 & & 213.449 & 0 & 0 & 0 \\
 & & & 111.515 & 0 & 0 \\
 & & & & 98.741 & 0 \\
 & & & & & 98.741
\end{bmatrix}
\mathbf{GPa}\,\mathbf{B}_\alpha \otimes \mathbf{B}_\beta
$$

$$
\mathbb{C}_E^{\text{Model}} =
\begin{bmatrix}
219.871 & 95.385 & 95.446 & 0.016 & -0.039 & -0.001 \\
 & 213.588 & 101.875 & -0.044 & -0.153 & -0.669 \\
 & & 213.527 & 0.028 & 0.192 & 0.670 \\
 & & & 111.751 & 0.948 & -0.216 \\
 & & & & 98.892 & 0.022 \\
 & & & & & 98.770
\end{bmatrix}
\mathbf{GPa}\,\mathbf{B}_\alpha \otimes \mathbf{B}_\beta
$$

Plane strain compression ($\xi = 0.0$, $\phi = 2.7$, $\mathbf{e}_2$ rolling direction, $\mathbf{e}_3$ normal direction):

$$
\mathbb{C}_E^{\text{Taylor}} =
\begin{bmatrix}
224.876 & 85.489 & 100.556 & 0 & 0 & 0 \\
 & 225.050 & 100.594 & 0 & 0 & 0 \\
 & & 209.493 & 0 & 0 & 0 \\
 & & & 108.993 & 0 & 0 \\
 & & & & 108.952 & 0 \\
 & & & & & 78.734
\end{bmatrix}
\mathbf{GPa}\,\mathbf{B}_\alpha \otimes \mathbf{B}_\beta
$$

$$
\mathbb{C}_E^{\text{Model}} =
\begin{bmatrix}
222.995 & 85.571 & 102.218 & 0.314 & -0.252 & -0.136 \\
 & 225.506 & 99.669 & 0.176 & 0.011 & -0.260 \\
 & & 208.981 & -0.490 & 0.240 & 0.396 \\
 & & & 107.339 & 0.561 & 0.016 \\
 & & & & 112.437 & 0.444 \\
 & & & & & 79.142
\end{bmatrix}
\mathbf{GPa}\,\mathbf{B}_\alpha \otimes \mathbf{B}_\beta
$$

Simple compression ($\xi = +0.5$, $\phi = 4.0$, $\mathbf{e}_1$ compression direction):

$$
\mathbb{C}_E^{\text{Taylor}} =
\begin{bmatrix}
219.262 & 95.684 & 95.684 & 0 & 0 & 0 \\
 & 213.475 & 101.873 & 0 & 0 & 0 \\
 & & 213.475 & 0 & 0 & 0 \\
 & & & 111.501 & 0 & 0 \\
 & & & & 99.192 & 0 \\
 & & & & & 99.192
\end{bmatrix}
\mathbf{GPa}\,\mathbf{B}_\alpha \otimes \mathbf{B}_\beta
$$

$$
\mathbb{C}_E^{\text{Model}} =
\begin{bmatrix}
219.636 & 96.202 & 95.015 & -0.155 & 0.077 & -0.204 \\
 & 212.175 & 102.396 & 0.065 & -0.046 & 0.138 \\
 & & 213.361 & 0.089 & -0.030 & 0.065 \\
 & & & 112.792 & 0.092 & -0.066 \\
 & & & & 98.030 & -0.219 \\
 & & & & & 100.404
\end{bmatrix}
\mathbf{GPa}\,\mathbf{B}_\alpha \otimes \mathbf{B}_\beta
$$

References

Adams, B.L., Mason, T.A., Olson, T., Sam, D.D., 1994. Theory of grain boundary structure effects on mechanical behavior. Materials Science Forum 157–162, 1731–1738.

Aleksandrov, K., Aisenberg, L., 1966. A method of calculating the physical constants of polycrystalline materials. Soviet Physics – Doklady 11, 323–325.

Alers, G., Liu, Y., 1966. Calculation of elastic anisotropy in rolled sheet. Trans. Met. Soc. AIME 236, 482–489.

Alers, G., Liu, Y., 1967. The nature of transition textures in copper. Trans. Met. Soc. AIME 239, 210–216.

Armstrong, P.J., Frederick C.O., 1966. A mathematical representation of the multiaxial Bauschinger effect. Report RD/B/N 731, 1966.

Asaro, R.J., Needleman, A., 1985. Overview no. 42: Texture development and strain hardening in rate dependent polycrystals. Acta Metall. 33, 923–953.

Bertram, A., 1992. Description of finite inelastic deformations. In: Benallal, A., Billardon, R., Marquis, D. (Eds.), Proceedings of MECAMAT'92 International Seminar on Multiaxial Plasticity, pp. 821–835.

Bertram, A., 1999. An alternative approach to finite plasticity based on material isomorphisms. Int. J. Plast. 15 (3), 353–374.

Bertram, A., Olschewski, J., 1991. Formulation of anisotropic linear viscoelastic constitutive laws by a projection method. In: Freed, A., Walker, K. (Eds.), High temperature constitutive modelling: Theory and Application, ASME, MD-vol. 26, AMD-vol. 121, pp. 129–137.

Boehler, J., 1987. Applications of Tensor Functions in Solid Mechanics. CISM Advanced School, Springer, Wien.

Boehler, J., Kirillov, A., Onat, E., 1994. On the polynomial invariants of the elasticity tensor. J. Elast. 34, 97–110.

Böhlke, T., Bertram, A., 1998. Simulation of texture development and induced anisotropy of polycrystals. In: Alturi, S., O'Donoghue, P., (Eds.), Proceedings of ICES'98, Modelling and Simulation Based Engineering, pp. 1390–1395.

Böhlke, T., Bertram, A., 2000. A minimum problem defining effective isotropic elastic properties. Z. Angew. Math. Mech. 80 (S2), S419–S420.

Bunge, H., 1993. Texture Analysis in Material Science. Cuviller Verlag, Göttingen.

Bunge, H.-J, 1968. Über die elastischen Konstanten kubischer Materialien mit beliebiger Textur. Kristall und Technik 3 (3), 431–438.

Bunge, H.-J., Roberts, W., 1969. Orientation distribution, elastic and plastic anisotropy in stabilized steel sheet. J. Appl. Cryst. 2, 116–128.

Cowin, S., 1989. Properties of the anisotropic elasticity tensor. Q. J. Mech. Appl. Math. 42, 249–266.

Cowin, S., 1990. Eigentensors of linear anisotropic elastic materials. Q. J. Mech. Appl. Math. 43, 15–41.

Davies, G., Goodwill, D., Kallend, J., 1972. Elastic and plastic anisotropy in sheets of cubic metals. Met. Trans. 3, 1627–1631.

Federov, F., 1968. Theory of Elastic Waves in Crystals. Plenum Press, New York.

Forte, S., Vianello, M., 1996. Symmetry classes for elasticity tensors. J. Elast. 43, 81–108.

Halmos, P., 1958. Finite-Dimensional Vector Spaces. D. van Nostrand Company, New York.

Harren, S., Asaro, R., 1989. Nonuniform deformations in polycrystals and aspects of the validity of the Taylor model. J. Mech. Phys. Solids 37 (2), 191–232.

Harren, S., Lowe, T., Asaro, R., Needleman, A., 1989. Analysis of large-strain shear in rate-dependent face-centred cubic polycrystals: correlation of micro- and macro-mechanics. Phil. Trans. R. Soc. Lond. A 328, 443–500.

Hill, R., 1952. The elastic behaviour of a crystalline aggregate. Proc. Phys. Soc. London A 65, 349–354.

Kallend, J., Davies, G., 1971. The elastic and plastic anisotropy of cold-rolled sheets of copper, gilding metal, and α-brass. J. Inst. Met. 5, 257-260.

Kocks, U., Tome, C., Wenk, H., 1998. Texture and Anisotropy: Preferred Orientations in Polycrystals and Their Effect on Materials Properties. Cambridge University Press, Cambridge.

Krempl, E., 1994. Deformation induced anisotropy. RPI-Report, MML 94-3, 1994.

Leffers, T., 1993. Microstructures, textures and deformation patterns at large strains. In: Teodosiu, C., Raphanel, J.L., Sidoroff, F. (Eds.), Proceedings of MECAMAT'91, pp. 73-86.

Lin, T.H., 1957. Analysis of elastic and plastic strains of a face-centered cubic crystal. J. Mech. Phys. Solids 5, 143–149.

Man, C.-S., 1995. On the correlation of elastic and plastic anisotropy in sheet metals. J. Elast. 39, 165–173.

Marsden, J., Hughes, T., 1983. Mathematical Foundations of Elasticity. Prentice-Hall, Englewood Cliffs NJ.

Matthies, S., Humbert, M., 1995. On the principle of a geometric mean of even-rank symmetric tensors for textured polycrystals. J. Appl. Cryst. 28, 254–266.

Mises, R., 1928. Mechanik der plastischen Formänderung bei Kristallen. Z. angew. Math. Mech. 8 (3), 161–185.

Morris, P., 1969. Averaging fourth-order tensors with weight functions. J. Appl. Phys. 40 (2), 447–448.

Nemat-Nasser, S., Hori, M., 1993. Micromechanics: Overall Properties of Heterogeneous Materials, North-Holland Series in Applied Mathematics and Mechanics, vol. 37. Elsevier, Amsterdam, 1993.

Oldroyd, J., 1950. Finite strains in an anisotropic continuum. Proc. R. Soc. London (A) 202, 345–358.

Reuss, A., 1929. Berechnung der Fließgrenze von Mischkristallen auf Grund der Plastizitätsbedingung für Einkristalle. Z. Angew. Math. Mech. 9, 49–58.

Rychlewski, J., 1995. Unconventional approach to linear elasticity. Arch. Mech. 47 (2), 149–171.

Rychlewski, J., Zhang, J., 1989. Anisotropy degree of elastic materials. Arch. Mech. 47 (5), 697–715.

Schouten, J., 1924. In: Der Ricci-Kalkül. Springer, New York, p. 1924.

Stickels, C., Mould, P., 1970. The use of Young's modulus for predicting the plastic-strain ratio of low-carbon steel sheets. Met. Trans. 1, 1303–1312.

Taylor, G.I., 1938. Plastic strain in metals. J. Inst. Metals 62, 307–324.

Truesdell, C., Noll, W., 1965. The Non-Linear Field Theories of Mechanics, Encyclopedia of Physics, vol. III/3. Springer, New York.

Voigt, W., 1910. Lehrbuch der Kristallphysik. Teubner Leipzig.

Weerts, J., 1933. Elastizität von Kupferblechen. Z. Metallk. 5, 101–103.

Wu, P., Neale, K., Giessen, E., 1996. Simulation of the behaviour of fcc polycrystals during reversed torsion. Int. J. Plast. 12 (9), 199–1219.

Zheng, Q.-S., Collins, I.F., 1998. The relationship between damage variables and evolution laws and microstructural and physical properties. Proc. R. Soc. London A 454, 1469–1498.